NASA TECHNICAL NOTE

NASA TN D-7054

NASA TN D-7054

ANALYSIS OF UNSTEADY THERMAL BOUNDARY LAYERS

by Roy W. Miller

Lewis Research Center

Cleveland, Ohio 44135

NATIONAL AERONAUTICS AND SPACE ADMINISTRATION • WASHINGTON, D. C. • NOVEMBER 1972

1. Report No.	2. Government Accession No.	3. Recipient's Catalog No.
NASA TN D-7054		

4. Title and Subtitle	5. Report Date
ANALYSIS OF UNSTEADY THERMAL BOUNDARY LAYERS	November 1972
	6. Performing Organization Code

7. Author(s)	8. Performing Organization Report No.
Roy W. Miller	E-6876
	10. Work Unit No. 503-10

9. Performing Organization Name and Address	11. Contract or Grant No.
Lewis Research Center National Aeronautics and Space Administration Cleveland, Ohio 44135	
	13. Type of Report and Period Covered
12. Sponsoring Agency Name and Address	Technical Note
National Aeronautics and Space Administration Washington, D. C. 20546	14. Sponsoring Agency Code

15. Supplementary Notes

16. Abstract

The velocity and temperature distribution in an unsteady thermal boundary layer is analyzed by an approximate integral method. The case of a flat plate in a free stream having small harmonic velocity oscillations about a steady mean value is treated in detail. The resulting velocity profiles agree with the available experimental data. These profiles are used to predict the thermal convection when the plate and the stream are at constant but different temperature levels. The flow oscillations cause harmonic temperature oscillations plus a small steady feedback effect which reduces the mean heat transfer to the plate. The amount of decrease is represented by a single coefficient, which is presented graphically.

17. Key Words (Suggested by Author(s))		18. Distribution Statement
Heat-transfer	Unsteady flow	Unclassified - unlimited
Boundary layers	Integral analysis	

19. Security Classif. (of this report)	20. Security Classif. (of this page)	21. No. of Pages	22. Price*
Unclassified	Unclassified	84	$3.00

* For sale by the National Technical Information Service, Springfield, Virginia 22151

Page Intentionally Left Blank

CONTENTS

ANALYSIS OF UNSTEADY THERMAL BOUNDARY LAYERS

by Roy W. Miller

Lewis Research Center

SUMMARY

The velocity and temperature distribution in an unsteady thermal boundary layer is analyzed by an approximate integral method. The case of a flat plate in a free stream having small harmonic velocity oscillations about a steady mean value is treated in detail. The resulting velocity profiles agree with the available experimental data. These profiles are used to predict the thermal convection when the plate and the stream are at constant but different temperature levels. The flow oscillations cause harmonic temperature oscillations plus a small steady feedback effect which reduces the mean heat transfer to the plate. The amount of decrease is represented by a single coefficient, which is presented graphically.

INTRODUCTION

Unsteady thermal boundary layers occur in many applications of unsteady flight, rotating blade motions, and nozzle flows. Previous analytical investigations of unsteady thermal boundary layers have been asymptotic in nature and thus apply to restricted ranges of interest (refs. 1 to 8). For flow with an oscillating free stream, solutions are asympotically valid for very low or very high frequency fluctuations. Results are generally limited to surface heat transfer, and detailed temperature distributions are not readily available. In this work, a general method of analysis is presented which will allow the calculation of approximate temperature profiles for a class of laminar two-dimensional flows with a wide range of applicability.

An integral method of analysis for unsteady laminar boundary-layer flow was recently investigated (refs. 9 and 10). That method basically consists of the following procedure:

(1) Obtain asymptotic solutions for limiting cases of the flow under consideration.

(2) Assume velocity profiles with sufficient generality to include the asymptotic solutions.

(3) Apply integral relations (velocity-weighted averages of the momentum equation) and compatibility conditions (normal derivatives of the momentum equation evaluated at the boundary) to determine the unknown velocity profile form parameters.

The present method of analysis for thermal boundary layers follows a similar procedure by utilizing the thermal energy equation as follows:

(1) Choose temperature profiles with sufficient generality to include known asymptotic solutions.

(2) Determine profile form parameters to satisfy temperature-weighted averages of the thermal energy equation.

The method is applied to the case of a flat plate in a free stream having small harmonic velocity oscillations about a steady mean value. Velocity profiles obtained by the method of references 9 and 10 are used as input for the thermal analysis. Those results were obtained by using integral relations and compatability conditions. In an attempt to improve the accuracy of previous results, the velocity profiles have been recomputed, using integral relations only, with results of the new computations presented herein.

INTEGRAL ANALYSIS OF UNSTEADY THERMAL BOUNDARY LAYERS

The integral method of analysis for unsteady thermal boundary layers is formulated here for incompressible flow over a flat plate with time-dependent free-stream velocity. In the analysis, it is assumed that the plate and the free stream are at constant but different temperatures. By establishing the general features of the method, other effects, such as prescribed heat flux, compressibility, or spatially varying pressure gradient, can later be included in the development.

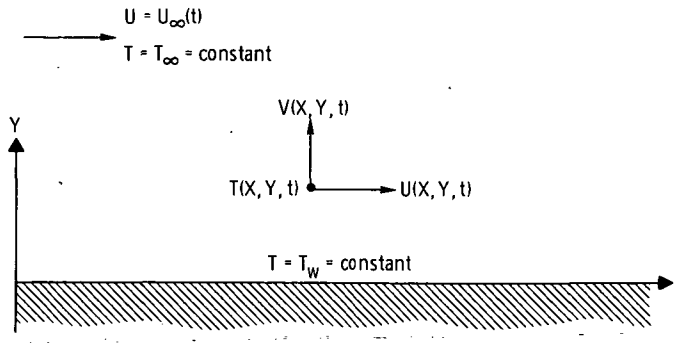

Figure 1. - Flat-plate boundary-layer configuration and nomenclature.

Boundary-Layer Equations

We consider the laminar two-dimensional incompressible flow and heat transfer for the flat-plate configuration shown in figure 1. The constant-temperature free stream has velocity which depends only on time and flows parallel to the isothermal plate. If viscous energy dissipation is neglected, the boundary-layer equations are

$$\frac{\partial U}{\partial X} + \frac{\partial V}{\partial Y} = 0 \tag{1}$$

$$\frac{\partial U}{\partial t} + U\frac{\partial U}{\partial X} + V\frac{\partial U}{\partial Y} = \nu\frac{\partial^2 U}{\partial Y^2} - \frac{1}{\rho}\frac{\partial P}{\partial X} \tag{2}$$

$$\frac{\partial P}{\partial Y} = 0 \tag{3}$$

$$\frac{\partial T}{\partial t} + U\frac{\partial T}{\partial X} + V\frac{\partial T}{\partial Y} = \alpha_{th}\frac{\partial^2 T}{\partial Y^2} \tag{4}$$

(Symbols are defined in appendix A.) The boundary conditions are as follows:

$$U(X,0,t) = 0 \tag{5}$$

$$V(X,0,t) = 0 \tag{6}$$

$$T(X,0,t) = T_w \tag{7}$$

$$U(X,Y,t) \to U_\infty(t) \quad \text{as } Y \to \infty \tag{8}$$

$$T(X,Y,t) \to T_\infty \quad \text{as } Y \to \infty \tag{9}$$

Since equation (3) implies constant pressure in the normal direction, the imposed pressure gradient is determined by evaluating equation (2) at the free stream, namely,

$$\frac{\partial U_\infty}{\partial t} = -\frac{1}{\rho}\frac{\partial P}{\partial X} \tag{10}$$

Equation (10), of course, applies for free-stream variations which depend on time alone.

Integral Relations

In references 9 and 10, a system of integral relations is derived for the unsteady boundary-layer flow. The momentum equation (2) is multiplied by U^k (k is a non-negative integer) and integrated in the Y-direction from the plate surface to the free stream. That is, a set of velocity-weighted averages of the momentum equation are formed. The resulting flow integral relations are as follows (see appendix B):

$$\frac{d}{dX}\int_0^\infty \frac{U}{k+1}\left(U^{k+1} - U_\infty^{k+1}\right)dY$$

$$= \begin{cases} \displaystyle\int_0^\infty \frac{\partial}{\partial t}(U_\infty - U)dY - \nu\left(\frac{\partial U}{\partial Y}\right)_{Y=0} & k = 0 \\ \displaystyle\int_0^\infty U^k \frac{\partial}{\partial t}(U_\infty - U)dY - \nu\int_0^\infty kU^{k-1}\left(\frac{\partial U}{\partial Y}\right)^2 dY & k > 0 \end{cases} \tag{11}$$

For $k = 0$, equation (11) gives the familiar momentum integral equation. The second equation with $k = 1$ is a mechanical energy balance for the boundary layer. No such interpretation can be made for $k > 1$.

A set of integral relations for the temperature can be obtained in a manner similar to the preceding by considering the thermal energy equation. First, introduce the dimensionless temperature ratio as follows:

$$\theta = \frac{T - T_w}{T_\infty - T_w} \tag{12}$$

With this definition, the values of dimensionless temperature at the wall and free stream are zero and 1, respectively. We next multiply equation (4) by θ^k and integrate in the Y-direction from the plate surface to the free stream. The result is

$$\int_0^\infty \theta^k \frac{\partial\theta}{\partial t}dY + \int_0^\infty \theta^k U \frac{\partial\theta}{\partial X}dY + \int_0^\infty \theta^k V \frac{\partial\theta}{\partial Y}dY = \alpha_{th}\int_0^\infty \theta^k \frac{\partial^2\theta}{\partial Y^2}dY \tag{13}$$

Upon imposing the flow continuity requirement and integrating by parts, we obtain the following set of temperature-weighted averages of the thermal energy equations (see appendix C):

$$\frac{d}{dX}\int_0^\infty \left[\frac{U}{k+1}\left(\theta^{k+1} - 1\right)\right]dY$$

$$= \begin{cases} -\displaystyle\int_0^\infty \frac{d\theta}{dt}\,dY - \alpha_{th}\left(\frac{\partial\theta}{\partial Y}\right)_{Y=0} & k = 0 \\ -\displaystyle\int_0^\infty \theta^k \frac{\partial\theta}{\partial t}\,dY - \alpha_{th}\, k \int_0^\infty \theta^{k-1}\left(\frac{\partial\theta}{\partial Y}\right)^2 dY & k > 0 \end{cases} \tag{14}$$

The first of these equations (k = 0) is the so-called heat-flux equation (refs. 11 and 12). The remaining equations (k > 0) have no known physical significance.

Method of Solution

The integral method described in references 9 and 10 utilizes the integral relations, equation (11), together with a set of compatibility conditions to determine approximate velocity profiles. Compatibility conditions are normal (Y) derivatives of the momentum equation (2), with the result evaluated at the plate surface. The U-velocity component is taken to vary exponentially in the Y-direction, and the X-dependence is included through velocity profile form parameters. The exponential form obviates the definition of a discrete boundary-layer thickness. The variable form parameters are required to satisfy the integral relations and the compatibility conditions. The integral relations demand that the profiles approximate the velocity values in some average sense across the boundary layer and that the compatibility conditions impose restrictions on the slope of the profiles at the wall.

The results in references 9 and 10 for oscillating flow over a flat plate show excellent agreement with experimental data (ref. 13) for the first-order unsteady effect. The second-order mean-flow profile approximation, at small values of the oscillation frequency, agrees only qualitatively with the exact asymptotic solution. Since the loss of

accuracy may have been caused by the nature of the compatibility conditions, the analysis presented herein employs the integral relations alone to determine the profile parameters.

The thermal boundary layer is computed in a manner similar to the flow. The assumed temperature profile parameters are determined in such a way that the thermal integral relations, equation (14), are satisfied.

FLOW OVER A FLAT PLATE WITH AN OSCILLATING FREE STREAM

In this section we conduct the detailed integral analysis of the flat-plate boundary layer for a free stream which performs small harmonic flow oscillations about a constant mean value. The flow is determined independently of heat transfer; in fact, the approximate solutions for the velocity boundary layer are later used in the thermal analysis.

Integral Relations

For the case of a free stream with small harmonic oscillations, of frequency ω and amplitude ϵU_0, about a steady mean value U_0, the free-stream velocity in equation (8) is expressed in complex form as follows:

$$U_\infty(t) = U_0(1 + \epsilon e^{i\omega t}) \tag{15}$$

The mathematical form of equation (15) suggests expansion of the local velocity in powers of the small amplitude parameter ϵ. Of course, the leading term (order ϵ^0) is the steady-flow boundary-layer velocity with free-stream velocity U_0. The ϵ^1 term corresponds to fluctuations, at frequency ω, which vary in amplitude and phase throughout the layer. Due to the quadratic nature of the boundary-layer equations, the ϵ^2 terms consist of oscillations at twice the fundamental frequency plus a steady feedback of the first-order oscillations on the mean flow (cf. ref. 10). Thus, we expand the U-velocity component, in dimensionless form, as follows:

$$u = u_0(x,y) + \epsilon u_1(x,y)e^{i\omega t} + \epsilon^2\left[\bar{u}_2(x,y) + \tilde{u}_2(x,y,t)\right] + \mathcal{O}(\epsilon^3) \tag{16}$$

where

$$\left.\begin{aligned} u &= \frac{U}{U_0} \\ x &= \frac{\omega X}{U_0} \\ y &= \sqrt{\frac{\omega}{\nu}}\, Y \end{aligned}\right\} \tag{17}$$

In equation (16), u_1 is the complex velocity component parallel to the plate with associated fluctuation magnitude and phase angle. The velocity component $\bar{u}_2$ is the contribution of the oscillations to the time-averaged flow.

We substitute equation (15) and the expansion, equation (16), into the flow integral relations, equation (11) in normalized form, and obtain the following set of integral relations:

Order ϵ^0:

$$\frac{d}{dx}\int_0^\infty \frac{u_0}{k+1}\left(u_0^{k+1} - 1\right)dy = \begin{cases} -\left(\dfrac{\partial u_0}{\partial y}\right)_{y=0} & k = 0 \\ -k\displaystyle\int_0^\infty u_0^{k-1}\left(\frac{\partial u_0}{\partial y}\right)^2 dy & k > 0 \end{cases} \tag{18}$$

Order ϵ^1:

$$\frac{d}{dx}\int_0^\infty \left(\frac{k+2}{k+1}\,u_1 u_0^{k+1} - u_0 - \frac{u_1}{k+1}\right)dy$$

$$= i\int_0^\infty (1-u_1)u_0^k\,dy - \begin{cases} \left(\dfrac{\partial u_1}{\partial y}\right)_{y=0} & k=0 \\ k\displaystyle\int_0^\infty \left[2u_0^{k-1}\left(\frac{\partial u_1}{\partial y}\right)\left(\frac{\partial u_0}{\partial y}\right) + (k-1)u_0^{k-2}u_1\left(\frac{\partial u_0}{\partial y}\right)^2\right]dy & k>0 \end{cases} \tag{19}$$

Order ϵ^2 (time-independent part):

$$\frac{d}{dx}\int_0^\infty \left[\frac{k+2}{4}u_0^k u_1 u_1^* + \frac{k+2}{k+1}\bar{u}_2 u_0^{k+1} - \frac{1}{2}\,Re\{u_1\} - \frac{\bar{u}_2}{k+1} - \frac{ku_0}{4}\right]dy$$

$$= \frac{k}{2}\,\mathcal{I}\left\{\int_0^\infty u_1 u_0^{k-1}\,dy\right\} - \begin{cases} \left(\dfrac{\partial \bar{u}_2}{\partial y}\right)_{y=0} & k=0 \\ k\displaystyle\int_0^\infty \left[2u_0^{k-1}\left(\frac{\partial u_0}{\partial y}\right)\left(\frac{\partial \bar{u}_2}{\partial y}\right) + \frac{u_0^{k-1}}{2}\left(\frac{\partial u_1}{\partial y}\right)\left(\frac{\partial u_1^*}{\partial y}\right) + \frac{k-1}{2}u_0^{k-2}\frac{\partial}{\partial y}(u_1 u_1^*)\left(\frac{\partial u_0}{\partial y}\right)\right. & k>0 \\ \qquad \left. + (k-1)u_0^{k-2}\bar{u}_2\left(\dfrac{\partial u_0}{\partial y}\right)^2 + \dfrac{(k-1)(k-2)}{4}u_0^{k-3}u_1 u_1^*\left(\dfrac{\partial u_0}{\partial y}\right)^2\right]dy & \end{cases} \tag{20}$$

where u_1^* denotes the complex conjugate of u_1.

We proceed with the integral analysis by assuming approximate forms for the velocity component (u_0, u_1, and $\bar{u}_2$) and then determining the form factors to satisfy the preceding integral relations.

Basic Mean Flow

It was mentioned earlier that the zeroth-order term in the velocity expansion (16) is the steady-flow boundary-layer velocity with constant free-stream velocity U_0. For the flat plate in a uniform stream, this basic mean flow is the familiar Blasius velocity profile u_B. This is, of course, a similarity solution in terms of the similarity variable, namely,

$$\eta = \frac{y}{\sqrt{x}} \tag{21}$$

Thus, the velocity component along the plate is

$$u_B = F_B'(\eta) \tag{22}$$

where F_B is the well-known Blasius stream function.

Note, from equations (19) and (20), that the zeroth-order velocity appears in the calculation of higher order terms. The use of tabulated values of the Blasius profile is inconvenient since the subsequent integral relations are algebraic in nature. Thus, we will compute algebraic approximations for the Blasius profile by the integral method of analysis.

Following references 9 and 10, consider four-parameter profile functions of the form

$$u_0 = 1 - e^{-A\eta}(1 + B\eta + C\eta^2 + D\eta^3) \tag{23}$$

These functions have the following desired behavior:

$$\left.\begin{aligned} u_0 &= 0 \quad \text{at} \quad y = 0 \\ u_0 &\to 1 \quad \text{as} \quad y \to \infty \end{aligned}\right\} \tag{24}$$

Four conditions are required to determine the four constants (A, B, C, and D). They are the four integral equations (18) with k = 0, 1, 2, and 3.

First, note the property

$$\frac{d}{d\zeta}\int_0^\infty \Omega(\eta)dy = \int_0^\infty \Omega(\eta)d\eta \tag{25}$$

where

$$\zeta = \sqrt{x} \tag{26}$$

Then, the four integral relations, equation (18) reduce to the following:

$$\int_0^\infty u_0(u_0 - 1)d\eta = -2\left(\frac{\partial u_0}{\partial \eta}\right)_{\eta=0} \tag{27}$$

$$\int_0^\infty u_0\left(u_0^2 - 1\right)d\eta = -4\int_0^\infty \left(\frac{\partial u_0}{\partial \eta}\right)^2 d\eta \tag{28}$$

$$\int_0^\infty u_0\left(u_0^3 - 1\right)d\eta = -12\int_0^\infty u_0\left(\frac{\partial u_0}{\partial \eta}\right)^2 d\eta \tag{29}$$

$$\int_0^\infty u_0\left(u_0^4 - 1\right)d\eta = -24\int_0^\infty u_0^2\left(\frac{\partial u_0}{\partial \eta}\right)^2 d\eta \tag{30}$$

Substituting the assumed profile forms, equation (23), into these relations and carrying out the indicated operations yields four algebraic equations for A, B, C, and D.

It is convenient to represent the profile approximation, and its derivative, in the following manner:

$$u_0 = f_1 - f_2 \tag{31}$$

$$\frac{du_0}{d\eta} = f_3 \tag{32}$$

where

$$f_i = e^{-s_i\eta} \sum_{m=1}^{4} h_{im}\eta^{m-1} \tag{33}$$

In equation (33) we have introduced the following arrays:

$$\left.\begin{aligned} s_i &= \begin{bmatrix} 0 \\ A \\ A \end{bmatrix} \\ h_{im} &= \begin{bmatrix} 1 & 0 & 0 & 0 \\ 1 & B & C & D \\ A - B & AB - 2C & AC - 3D & AD \end{bmatrix} \end{aligned}\right\} \tag{34}$$

By using these representations, integral terms of the type which appear in equations (27) to (30) can be given function definitions as follows:

$$F(I,J) = \int_0^{\infty} \sum_{i=1}^{4} \sum_{j=1}^{4} \eta^{i+j-2} e^{-(s_I+s_J)} h_{Ii} h_{Jj}\, d\eta \tag{35}$$

We recall the following integration formula:

$$\int_0^{\infty} Z^n e^{-C_0 Z}\, dZ = \frac{n!}{C_0^{n+1}} \tag{36}$$

where n is a nonnegative integer and $C_0 > 0$. Then, the function definitions reduce to the following:

$$F(I, J) = \frac{h_{Ii} h_{Jj} [(i + j - 2)!]}{(s_I + s_J)^{i+j-1}} \qquad \text{Sum on } i \text{ and } j \text{ from 1 to 4} \tag{37}$$

The F notation is readily extended for additional subscripts, and the following simplified form for equations (27) to (30) is obtained:

$$[F(2, 1) - F(2, 2)] - 2(A - B) = 0 \tag{38}$$

$$[2F(2, 1) - 3F(2, 2) + F(2, 2, 2)] - 4[F(3, 3)] = 0 \tag{39}$$

$$[3F(2, 1) - 6F(2, 2) + 4F(2, 2, 2) - F(2, 2, 2, 2)] - 12[F(3, 3) - F(3, 3, 2)] = 0 \tag{40}$$

$$[4F(2, 1) - 10F(2, 2) + 10F(2, 2, 2) - 5F(2, 2, 2, 2) + F(2, 2, 2, 2, 2)]$$

$$- 24[F(3, 3) - 2F(3, 3, 2) + F(3, 3, 2, 2)] = 0 \tag{41}$$

The form factors were computed to satisfy equations (38) to (41) by applying the computational scheme outlined in appendix D. The resulting values are as follows:

$$\begin{bmatrix} A \\ B \\ C \\ D \end{bmatrix} = \begin{bmatrix} 1.9059 \\ 1.5709 \\ 0.8159 \\ 1.1655 \end{bmatrix} \tag{42}$$

Values of the corresponding velocity profile are presented in table I, together with the Blasius profile values and the reference 9 results based on three integral relations plus one compatibility condition. The present values are closer to the Blasius data, except near the plate surface.

Velocity Oscillations

We compute the first-order oscillating component of velocity by following the procedure of references 9 and 10: that is, obtain asymptotic solutions for the flow under

TABLE I. - COMPARISON OF FOUR-PARAMETER PROFILE

APPROXIMATIONS WITH THE BLASIUS PROFILE

Similarity variable, $\eta = y/\zeta$	Blasius value	Three integral relations (ref. 9 result)		Four integral relations	
		Value	Percent error	Value	Percent error
0.20	0.06641	0.06579	-0.94	0.07368	10.95
.40	.13277	.12888	-2.93	.14456	8.88
.60	.19894	.19097	-4.00	.20710	4.10
.80	.26471	.25414	-3.99	.26518	.18
1.00	.32979	.31923	-3.20	.32312	-2.02
1.20	0.39378	0.38584	-2.02	0.38311	-2.71
1.40	.45627	.45273	-.78	.44526	-2.41
1.60	.51676	.51833	.30	.50833	-1.63
1.80	.57477	.58112	1.10	.57054	-.74
2.00	.62977	.63985	1.60	.63014	.06
2.20	0.68132	0.69362	1.81	0.68566	0.64
2.40	.72899	.74194	1.78	.73613	.98
2.60	.77246	.78462	1.57	.78099	1.10
2.80	.81152	.82176	1.26	.82010	1.06
3.00	.84605	.85364	.90	.85364	.90
3.20	0.87609	0.88068	0.52	0.88195	0.67
3.40	.90177	.90337	.18	.90555	.42
3.60	.92333	.92223	-.12	.92498	.18
3.80	.94112	.93776	-.36	.94082	-.03
4.00	.95552	.95045	-.53	.95360	-.20
4.20	0.96696	0.96075	-0.64	0.96383	-0.32
4.40	.97587	.96905	-.70	.97195	-.40
4.60	.98269	.97570	-.71	.97836	-.44
4.80	.98779	.98099	-.69	.98338	-.45
5.00	.99155	.98519	-.64	.98729	-.43
5.20	0.99425	0.98850	-0.58	0.99031	-0.40
5.40	.99616	.99110	-.51	.99265	-.35
5.60	.99748	.99313	-.44	.99444	-.30
5.80	.99838	.99472	-.37	.99581	-.26
6.00	.99898	.99595	-.30	.99685	-.21
6.20	0.99937	0.99690	-0.25	0.99764	-0.17
6.40	.99961	.99763	-.20	.99824	-.14
6.60	.99977	.99820	-.16	.99868	-.11
6.80	.99987	.99863	-.12	.99902	-.08
7.00	.99992	.99896	-.10	.99927	-.06

consideration; assume profiles with sufficient generality to include the asymptotic solutions; and determine the unknown profile form parameters to satisfy the flow integral relations.

Quasi-steady flow. - The asymptotic solution of interest for the plate in an oscillating stream is the so-called "quasi-steady" flow. For the limiting case of very low-frequency fluctuations, the boundary-layer response is quasi-steady at the prevailing value of the free-stream velocity. The solution then follows the Blasius form based on the instantaneous free-stream velocity, that is,

$$U_Q = U_Q(1 + \epsilon e^{i\omega t}) F'_B\left(\frac{y}{\sqrt{x}}\sqrt{1 + \epsilon e^{i\omega t}}\right) \tag{43}$$

We expand equation (43) in a Taylor series for small free-stream perturbations and identify the first-order quasi-steady velocity as

$$u_{1Q} = F'_B(\eta) + \frac{1}{2}\eta F''_B(\eta) \tag{44}$$

An approximation to the quasi-steady flow velocity is obtained by the integral method by first assuming the four-parameter profile form as follows:

$$u_{1q} = 1 - e^{-a\eta}(1 + b\eta + c\eta^2 + d\eta^3) \tag{45}$$

The constants a, b, c, and d are obtained by demanding that u_{1q} satisfy the four integral relations, equations (19) with k = 0, 1, 2, and 3.

Since the quasi-steady velocity depends on the similarity variable, equations (19) will reduce to algebraic relations in a manner similar to the Blasius flow approximation. We extend the previous matrix definitions to include the quasi-steady approximation and its derivative, that is,

$$u_{1q} = f_1 - f_4 \tag{46}$$

$$\frac{du_{1q}}{d\eta} = f_5 \tag{47}$$

and

$$s_i = \begin{bmatrix} 0 \\ A \\ A \\ a \\ a \end{bmatrix} \qquad h_{im} = \begin{bmatrix} 1 & 0 & 0 & 0 \\ 1 & B & C & D \\ A - B & AB - 2C & AC - 3D & AD \\ 1 & b & c & d \\ a - b & ab - 2c & ac - 3d & ad \end{bmatrix} \tag{48}$$

Then, the first-order flow integral relations can be reduced to the following:

$$[F(4) + F(2) - 2F(4,2)] - 2(a - b) = 0 \tag{49}$$

$$[2F(4) + 4F(2) - 6F(4,2) - 3F(2,2) + 3F(4,2,2)] - 8[F(5,3)] = 0 \tag{50}$$

$$[3F(4) + 9F(2) - 12F(4,2) - 12F(2,2) + 12F(4,2,2) + 4F(2,2,2) - 4F(4,2,2,2)]$$

$$- 12[2F(5,3) + F(3,3) - 2F(5,3,2) - F(4,3,3)] = 0 \tag{51}$$

$$[4F(4) + 16F(2) - 20F(4,2) - 30F(2,2) + 30F(4,2,2) + 20F(2,2,2) - 20F(4,2,2,2)$$

$$- 5F(2,2,2,2) + 5F(4,2,2,2,2)] - 48[F(5,3) + F(3,3) - 2F(5,3,2)$$

$$- F(4,3,3) - F(3,3,2) + F(5,3,2,2) + F(4,3,2,2)] = 0 \tag{52}$$

The profile form parameters were computed from equations (49) to (52) by the method of appendix D with the following result:

$$\begin{bmatrix} a \\ b \\ c \\ d \end{bmatrix} = \begin{bmatrix} 1.40244 \\ 0.91137 \\ 0.68585 \\ -0.53889 \end{bmatrix} \tag{53}$$

The associated profile is shown in figure 2. Also shown in figure 2 are the exact quasi-steady solution and the reference 9 results obtained by using three integral relations plus one compatibility condition. Some improvement was realized by applying the fourth integral relation.

Stokes flow solution. - Another asymptotic solution, which will later be of interest,

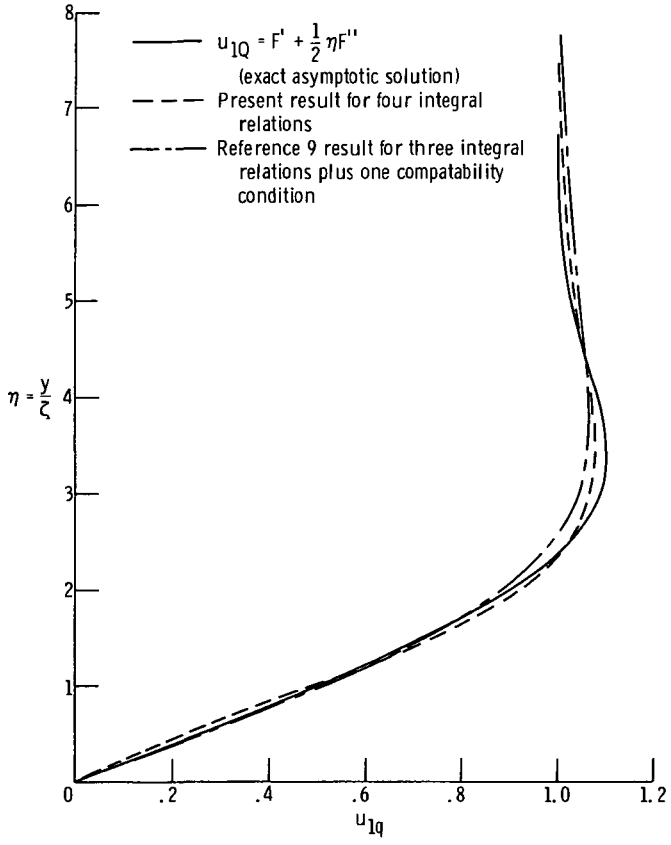

Figure 2. - Four-parameter profile approximations for first-order quasi-steady flow.

is the Stokes flow solution for large values of $\zeta = \sqrt{\omega X/U_0}$. For this limiting case, viscous and unsteady effects dominate and the flow depends only on y. The well-known Stokes flow result is the following (cf. ref. 14):

$$u_{1S} = 1 - e^{-\sqrt{i}\,y} \tag{54}$$

Profile factors. - The general first-order velocity profile approximation, which applies for all frequency values, is assumed to be of the following form:

$$u_1 = 1 - e^{-\alpha y}(1 + \beta y + \gamma y^2 + \delta y^3) \tag{55}$$

where the complex profile form factors (α, β, γ, and δ) are functions of the variable $\zeta = \sqrt{\omega X/U_0}$. Equation (55) shows the desired behavior, which is zero value at the plate

surface and approaching unity at the free stream. Of course, for lower frequencies the independent variables combine as the similarity variable and equation (55) yields the quasi-steady approximation. Also the Stokes flow, equation (54) is a specialized form of equation (55).

We determine the form factors in equation (55) to satisfy the integral conditions (19) The integration over y is carried out as done previously, by introducing appropriate function definitions. However, since the general dependence of u_1 on x is not known, the integral relations will result in a set of first-order ordinary differential equations for α, β, γ, and δ. The resulting set of nonlinear equations is of the following standard form:

$$P_{i1}\frac{d\alpha}{d\zeta} + P_{i2}\frac{d\beta}{d\zeta} + P_{i3}\frac{d\gamma}{d\zeta} + P_{i4}\frac{d\delta}{d\zeta} = R_i \qquad i = 1,\ 2,\ 3,\ 4 \tag{56}$$

The coefficients in equation (56) depend on α, β, γ, δ, and ζ. Refer to appendix E for the detailed coefficients.

Since equations (56) are linear in the form parameter slopes, we can solve for these values by applying Cramer's rule and obtain the following results:

$$\left.\begin{aligned}
\frac{d\alpha}{d\zeta} &= \pi_1(\alpha,\beta,\gamma,\delta,\zeta) \\
\frac{d\beta}{d\zeta} &= \pi_2(\alpha,\beta,\gamma,\delta,\zeta) \\
\frac{d\gamma}{d\zeta} &= \pi_3(\alpha,\beta,\gamma,\delta,\zeta) \\
\frac{d\delta}{d\zeta} &= \pi_4(\alpha,\beta,\gamma,\delta,\zeta)
\end{aligned}\right\} \tag{57}$$

These complex equations are equivalent to eight real first-order differential equations; and thus, eight initial values are required to obtain the solution. The eight values are the real and imaginary parts of α, β, γ, and δ evaluated at the low-frequency limit (i.e., $\zeta \to 0$). The real parts of the form parameters are associated with the quasi-steady approximation (eq. (45)), whence

$$\begin{bmatrix} \alpha_r \\ \beta_r \\ \gamma_r \\ \delta_r \end{bmatrix} \sim \begin{bmatrix} a/\zeta \\ b/\zeta \\ c/\zeta^2 \\ d/\zeta^3 \end{bmatrix} \quad \text{as } \zeta \to 0 \tag{58}$$

In fact, the quasi-steady behavior can be identified as the leading real term of an expansion for small ζ, namely,

$$\left.\begin{aligned} \alpha_q &\sim \frac{a}{\zeta}\left(1 + a_1\zeta + a_2\zeta^2 + \ldots\right) + i\tilde{a}\zeta\left(1 + \tilde{a}_1\zeta + \tilde{a}_2\zeta^2 + \ldots\right) \\ \beta_q &\sim \frac{b}{\zeta}\left(1 + b_1\zeta + b_2\zeta^2 + \ldots\right) + i\tilde{b}\zeta\left(1 + \tilde{b}_1\zeta + \tilde{b}_2\zeta^2 + \ldots\right) \\ \gamma_q &\sim \frac{c}{\zeta^2}\left(1 + c_1\zeta + c_2\zeta^2 + \ldots\right) + i\tilde{c}\left(1 + \tilde{c}_1\zeta + \tilde{c}_2\zeta^2 + \ldots\right) \\ \delta_q &\sim \frac{d}{\zeta^3}\left(1 + d_1\zeta + d_2\zeta^2 + \ldots\right) + i\frac{\tilde{d}}{\zeta}\left(1 + \tilde{d}_1\zeta + \tilde{d}_2\zeta^2 + \ldots\right) \end{aligned}\right\} \tag{59}$$

Now, the initial behavior of the imaginary parts of the form parameters can be obtained by substituting the expansions (59) into equations (56) and retaining the dominant imaginary terms. Upon solving the resulting equations by the method of appendix D, we obtain the following:

$$\begin{bmatrix} \alpha_i \\ \beta_i \\ \gamma_i \\ \delta_i \end{bmatrix} \sim \begin{bmatrix} 0.32372\ \zeta \\ -0.51773\ \zeta \\ 0.07723 \\ -0.51783/\zeta \end{bmatrix} \quad \zeta \to 0 \tag{60}$$

The set of equations (57) was solved numerically by using the Runge-Kutta formulas listed in appendix F. The initial values were obtained by evaluating equations (58) and (60) at $\zeta = 0.01$ - a starting value for which the quasi-steady solution was reproduced. Results for the real and imaginary parts of the form parameters are shown graphically in figures 3 and 4, respectively. The computation was terminated when subsequent calculation showed that the Stokes flow had been approximately achieved.

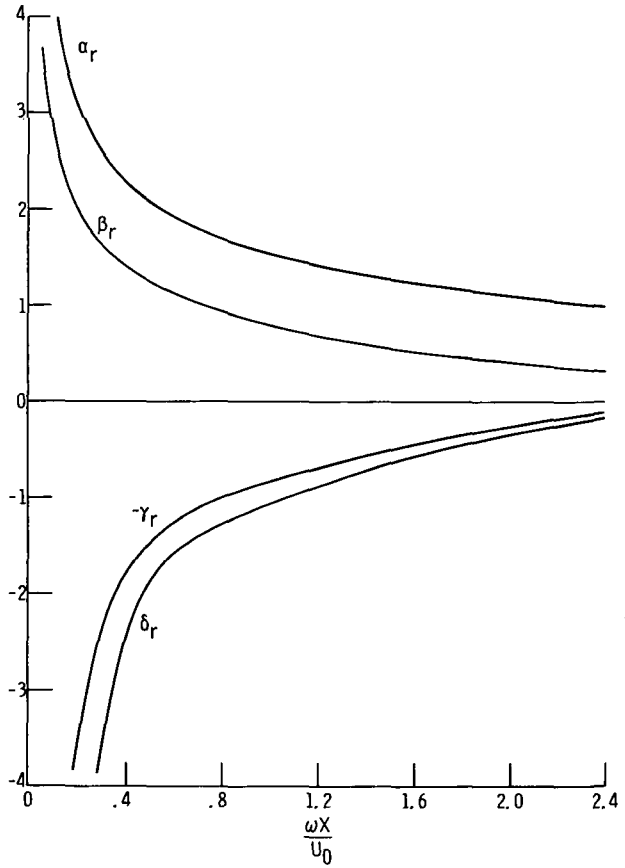

Figure 3. - Real parts of first-order velocity profile form factors.

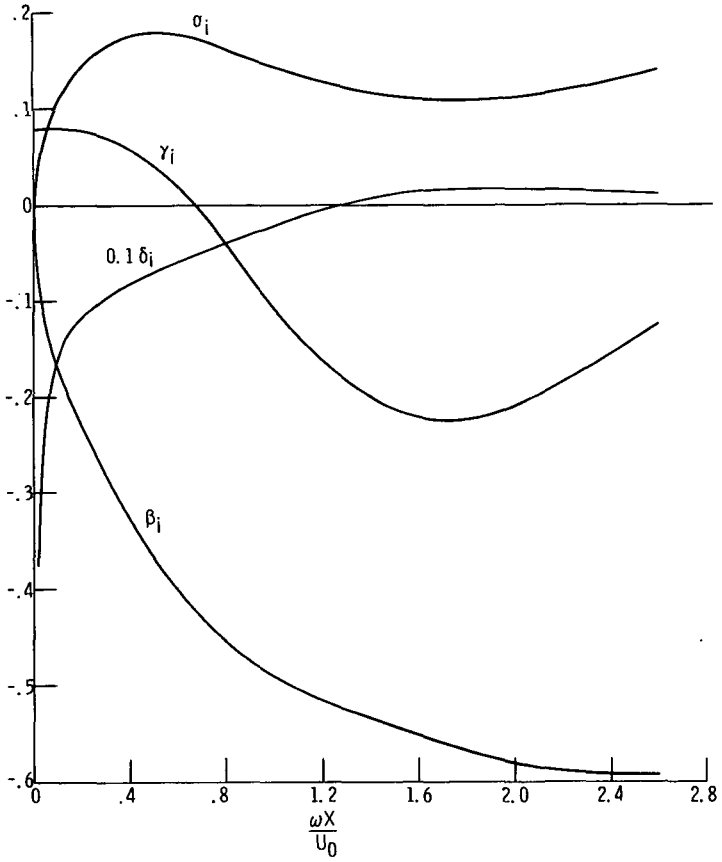

Figure 4. - Imaginary parts of first-order velocity profile form factors.

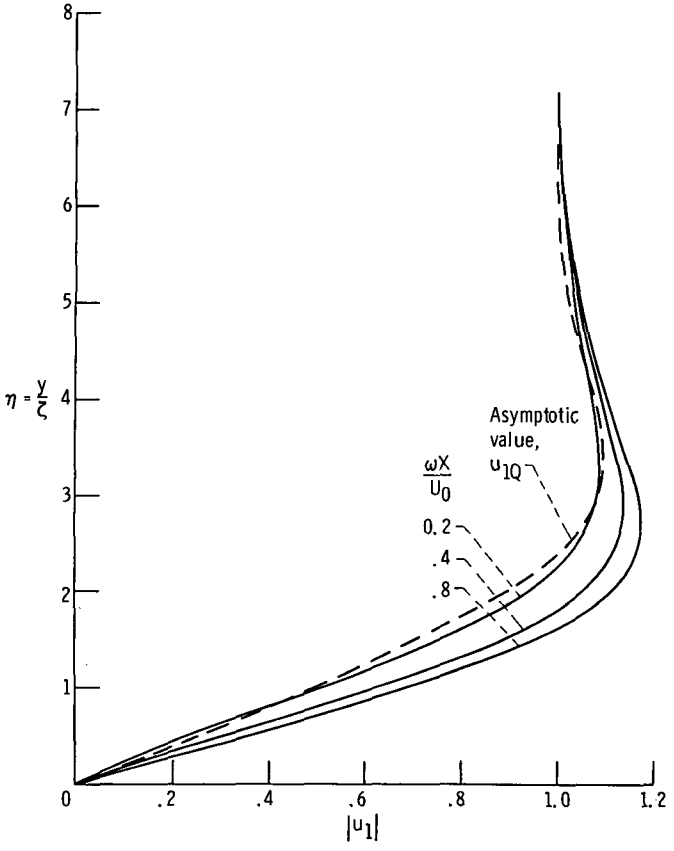

Figure 5. - Development of first-order velocity magnitude for small values of ζ.

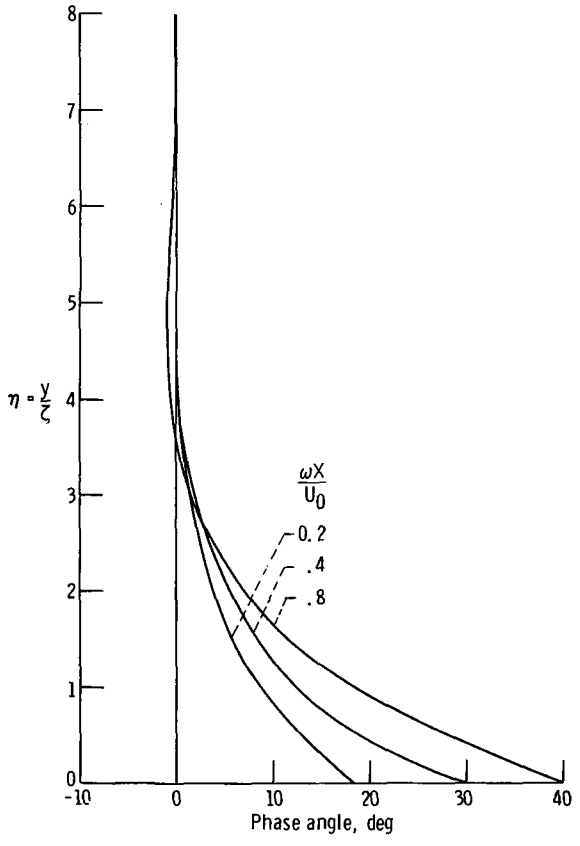

Figure 6. - Development of first-order velocity phase angle for small values of ζ.

Profile results. - After the profile-form factors have been determined, the first-order velocity profiles are readily computed by using equation (55). We denote the magnitude of fluctuations by $|u_1|$, and a positive phase angle represents a phase lead with respect to the free-stream variation.

The development of the first-order velocity for small values of $\zeta = \sqrt{\omega X/U_0}$ is shown in figures 5 and 6. Results are plotted against the similarity variable η to show the departure from quasi-steady flow. Recall that the quasi-steady fluctuations are "in phase" throughout the flow field. The unsteady acceleration force applies simultaneously throughout the flow field. The slower moving fluid near the wall responds to this force faster than the main stream, thus causing a phase advance near the wall.

Profiles of the first-order velocity for large values of $\zeta = \sqrt{\omega X/U_0}$ are presented in figures 7 and 8. The variation as a function of y is of interest here; and, results show that the Stokes flow limit is approximately approached at $\zeta^2 = 3$.

Computed first-order velocity results are compared with the data of Hill and Stenning (ref. 13) in figures 9 and 10. Again, for small values of $\omega X/U_0$, results are plotted against η; and, for large values of $\omega X/U_0$, the normal coordinate $y/\sqrt{2}$ is used. In all cases the agreement between present and experimental results is very good.

The frictional drag is related to the normal derivative of the velocity, with the result evaluated at the wall, that is,

$$\left(\frac{\partial u}{\partial y}\right)_{y=0} = \left(\frac{\partial u_0}{\partial y}\right)_{y=0} + \epsilon \left(\frac{\partial u_1}{\partial y}\right)_{y=0} e^{i\omega t} + \mathcal{O}(\epsilon^2) \tag{61}$$

The first-order term again has components in phase and out of phase with the free-stream oscillations. Also, since the first-order term is oscillatory, there is no net first-order contribution to the drag in the time-average sense.

We define a first-order wall shear stress coefficient, which is normalized by the magnitude of the Blasius shear, as follows:

$$C_{\tau 1} = \frac{\left(\frac{\partial u_1}{\partial y}\right)_{y=0}}{\left(\frac{\partial u_B}{\partial y}\right)_{y=0}} \tag{62}$$

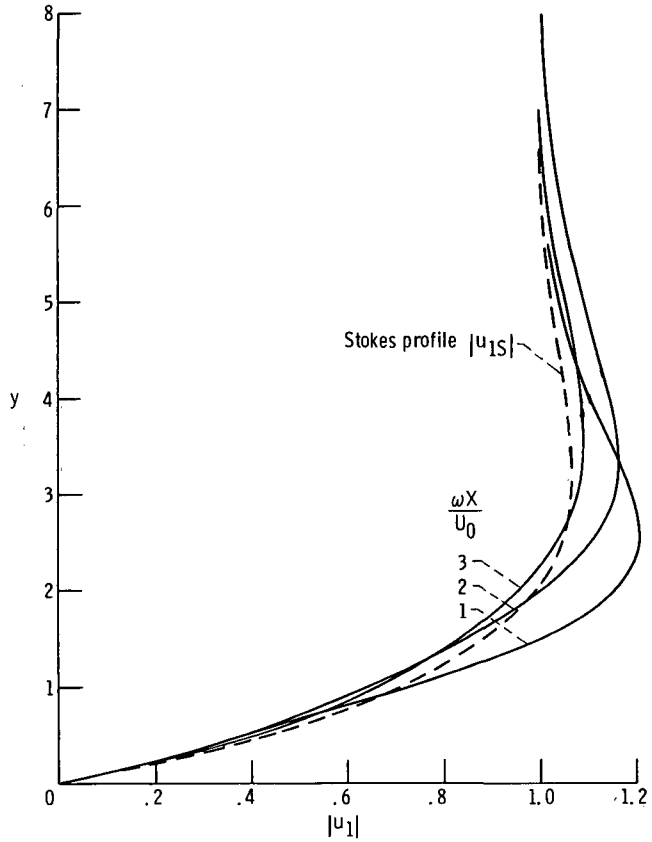

Figure 7. - Development of the first-order velocity magnitude for large values of ζ.

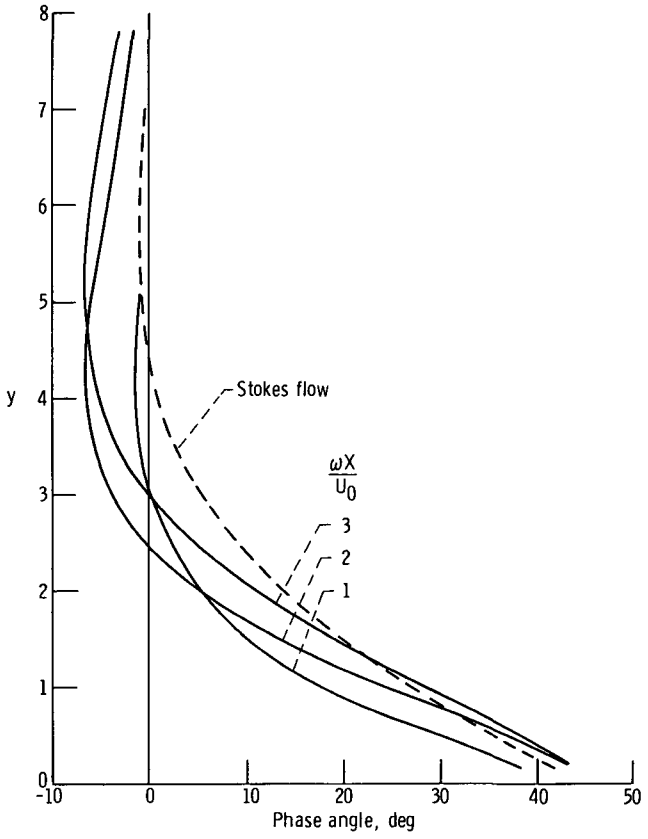

Figure 8. - Development of first-order velocity phase angle for large values of ζ.

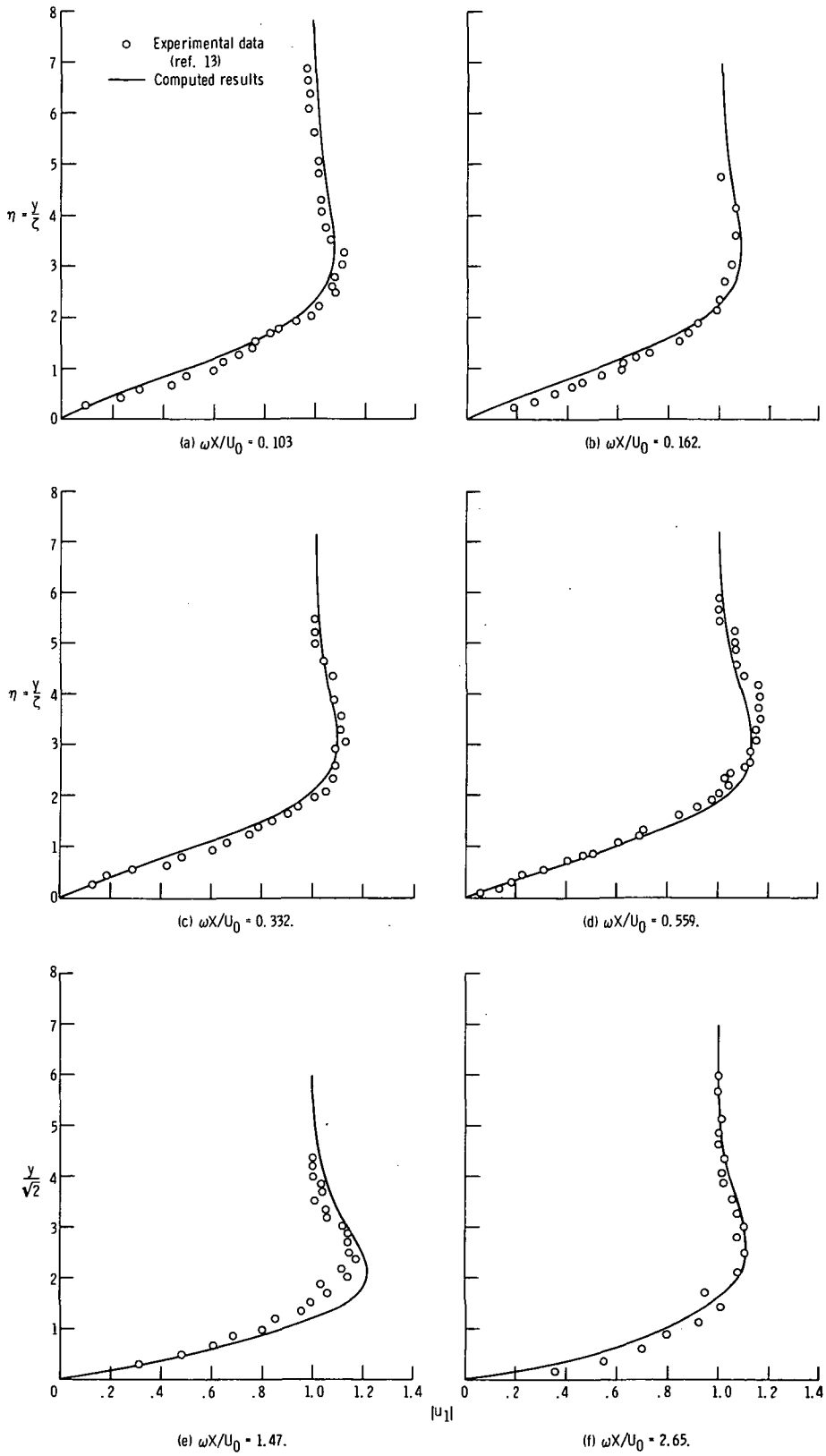

(a) $\omega X/U_0 = 0.103$

(b) $\omega X/U_0 = 0.162$.

(c) $\omega X/U_0 = 0.332$.

(d) $\omega X/U_0 = 0.559$.

(e) $\omega X/U_0 = 1.47$.

(f) $\omega X/U_0 = 2.65$.

Figure 9. - Magnitude of first-order velocity oscillations.

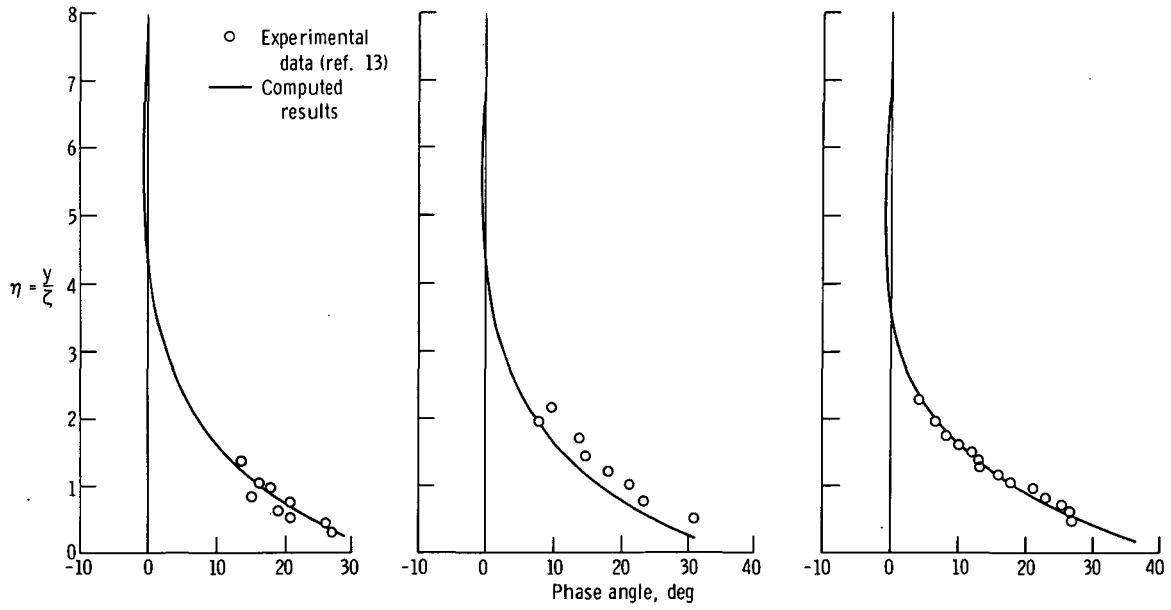

(a) $\omega X/U_0 = 0.472$. (b) $\omega X/U_0 = 0.522$. (c) $\omega X/U_0 = 0.830$.

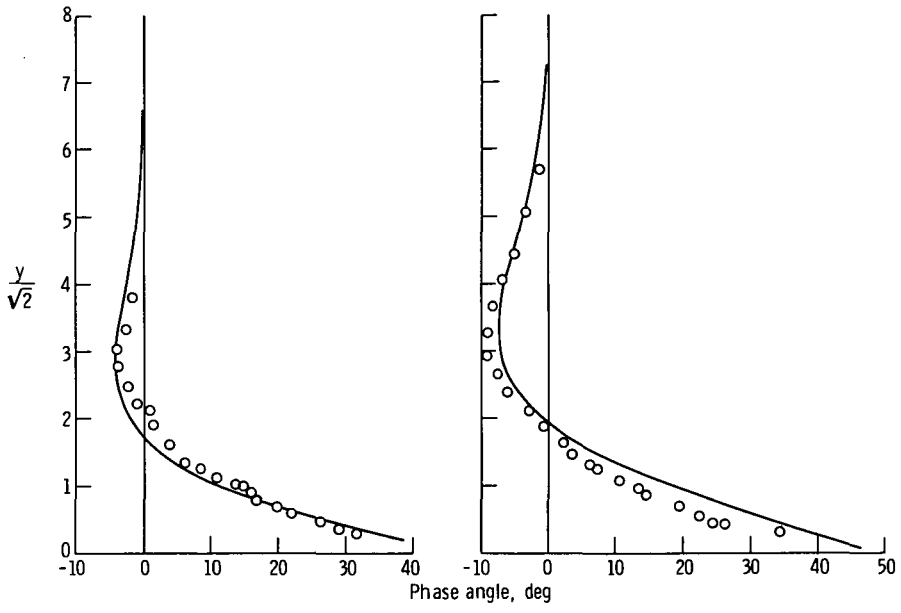

(d) $\omega X/U_0 = 1.48$. (e) $\omega X/U_0 = 2.49$.

Figure 10. - Phase angle of first-order velocity oscillations.

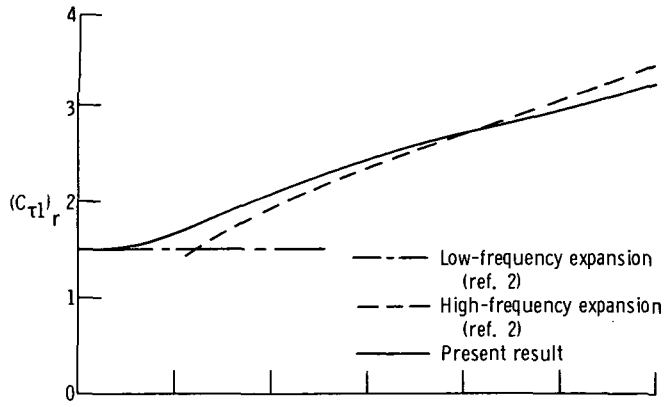

(a) Real part.

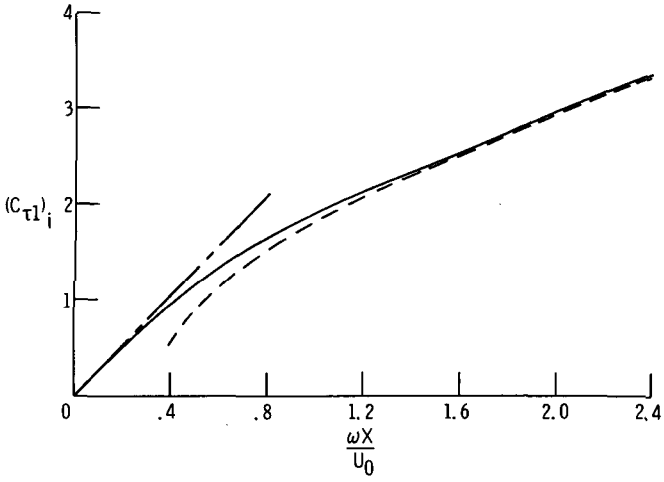

(b) Imaginary part.

Figure 11. - First-order wall shear stress coefficient.

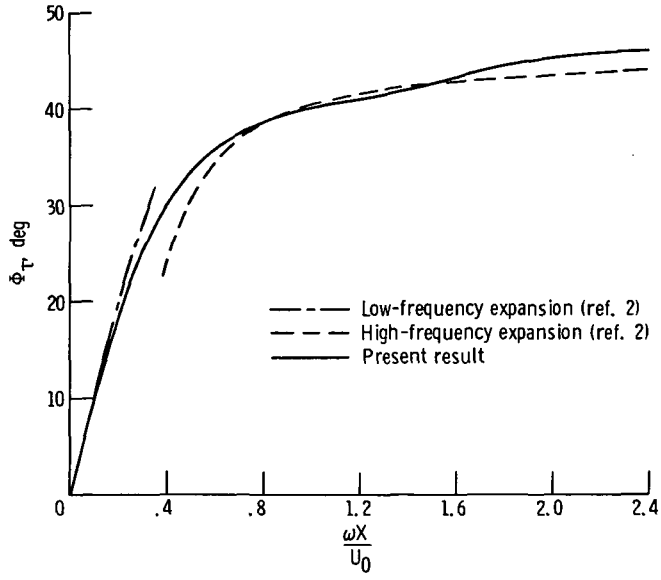

Figure 12. - Phase angle of first-order wall shear stress coefficient.

Values of the shear coefficient components and the associated phase angle Φ_τ are shown in figures 11 and 12. The present results span the asymptotic limits given by Illingworth in reference 2.

Effect of Oscillations on the Time-Average Flow

We complete the flow analysis by computing the steady second-order velocity profile, that is, the feedback of the first-order oscillations on the steady mean flow. Again we consider a limiting-case solution and then apply the integral method of analysis.

Quasi-steady flow. - The asymptotic solution for quasi-steady flow (low-frequency limit) is obtained by continuing the expansion of equation (43). The resulting second-order quasi-steady velocity is as follows:

$$\bar{u}_{2Q} = \frac{\eta}{32} F_B''\left(6 - \eta F_B'\right) \tag{63}$$

This solution is indicated by the solid-line curve in figure 13.

We consider approximate quasi-steady profile forms as follows:

$$\bar{u}_{2q} = e^{-p\eta}(q\eta + r\eta^2 + s\eta^3) \tag{64}$$

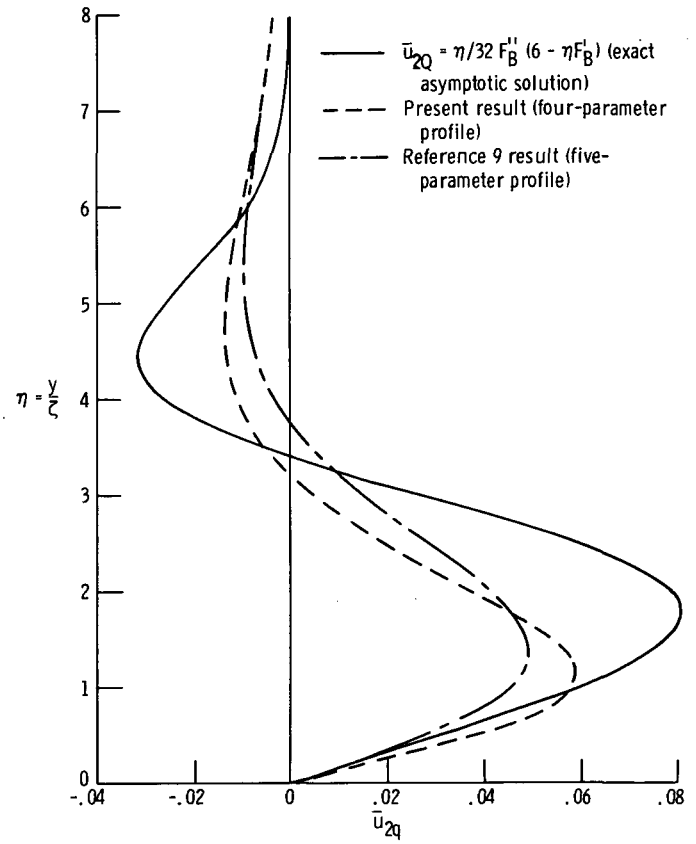

Figure 13. - Second-order quasi-steady velocity profile approximation.

These forms have zero values at the wall and free stream, and they admit an intermediate zero for certain values of the coefficients.

The constant profile factors in equation (64) are determined in a straightforward manner by the integral method. We first expand the array definitions (48) as follows:

$$[f_i] = \begin{bmatrix} 1 \\ 1 - u_0 \\ du_0/d\eta \\ 1 - u_{1q} \\ du_{1q}/d\eta \\ \bar{u}_{2q} \\ d\bar{u}_{2q}/d\eta \end{bmatrix} \qquad [s_i] = \begin{bmatrix} 0 \\ A \\ A \\ a \\ a \\ p \\ p \end{bmatrix} \qquad [h_{im}] = \begin{bmatrix} 1 & 0 & 0 & 0 \\ 1 & B & C & D \\ A - B & AB - 2C & AC - 3D & AD \\ 1 & b & c & d \\ a - b & ab - 2c & ac - 3d & ad \\ 0 & q & r & s \\ q & 2r - pq & 3s - pr & -ps \end{bmatrix} \tag{65}$$

Then when the F-function notation is introduced, the four integral relations with $k = 0, 1, 2,$ and 3, equations (20), are reduced to

$$[F(4,4) - F(4,1)] + 2[F(6,1) - 2F(6,2)] + 4q = 0 \tag{66}$$

$$[3F(4,4) - 4F(4,1) + 6F(4,2) - 3F(4,4,2) - 2F(2,1)] + 2[F(6,1) - 6F(6,2) + 3F(6,2,2) + 8F(7,3) + 2F(5,5)] = 0 \tag{67}$$

$$3[2F(2,2) - 3F(2,1) - 3F(4,1) + 8F(4,2) + 2F(4,4) - 4F(4,4,2) - 4F(4,2,2) + 2F(4,4,2,2)] + 12[4F(7,3) + F(5,5) - 4F(7,3,2) - F(5,5,2) + 2F(5,3) - 2F(5,4,3) + 2F(6,3,3)] + 2[12F(6,2,2) - 12F(6,2) - 3F(6,1) - 4F(6,2,2,2)] = 0 \tag{68}$$

$$5[3F(2,2) - F(2,2,2) + 6F(4,2) - 6F(4,2,2) + 2F(4,2,2,2) + F(4,4) - 3F(4,4,2) + 3F(4,4,2,2) - F(4,4,2,2,2)] - 8F(4,1) + 4F(6,1) - 12F(2,1) + 12[4F(7,3) + F(5,5)] + 5[F(6,2,2,2,2) - 4F(6,2,2,2) + 6F(6,2,2) - 4F(6,2)] + 12[4F(7,3,2,2) + F(5,5,2,2) + F(3,3) - 2F(4,3,3) + F(4,4,3,3) - 8F(7,3,2) - 2F(5,5,2)] + 48[F(5,3) - F(5,4,3) - F(5,3,2) + F(5,4,3,2) + F(6,3,3) - F(6,3,3,2)] = 0 \tag{69}$$

where the property expressed by equation (25) has been observed.

The solution of equations (66) to (69) is obtained as outlined in appendix D, with the result as follows:

$$\begin{bmatrix} p \\ q \\ r \\ s \end{bmatrix} = \begin{bmatrix} 1.06634 \\ 0.063332 \\ 0.161027 \\ -0.056376 \end{bmatrix} \tag{70}$$

Values of the corresponding quasi-steady profile approximation are shown in figure 13. The result of reference 9 is also shown for a five-parameter profile with coefficients determined by applying three integral and two compatibility conditions. The use of only integral relations gives a better approximation, even though the number of profile parameters is one less.

Profile factors. - We generalize equation (64), to apply for all frequency values, as follows:

$$\bar{u}_2 = e^{-\varphi y}(\psi y + \mu y^2 + \lambda y^3) \tag{71}$$

The profile-form factors (φ, ψ, μ, and λ) are, of course, functions of the variable $\zeta = \sqrt{\omega X/U_0}$. We identify the limiting behavior of the functions as the quasi-steady result, namely,

$$\begin{bmatrix} \varphi_q \\ \psi_q \\ \mu_q \\ \lambda_q \end{bmatrix} \sim \begin{bmatrix} p/\zeta \\ q/\zeta \\ r/\zeta^2 \\ s/\zeta^3 \end{bmatrix} \quad \text{as } \zeta \to 0 \tag{72}$$

The computation of the form factors follows the first-order flow analysis: that is, substitute the profile forms into equation (20) with $k = 0, 1, 2,$ and 3; introduce the appropriate function notation and carry out the integration over y; and rewrite the resulting differential equations in the standard form. The result is

$$P_{i1}\frac{d\varphi}{d\zeta} + P_{i2}\frac{d\psi}{d\zeta} + P_{i3}\frac{d\mu}{d\zeta} + P_{i4}\frac{d\lambda}{d\zeta} = R_i \qquad i = 1, 2, 3, 4 \tag{73}$$

where coefficients P_{ij} and R_i are listed in appendix E.

The first-order differential equations (73), with the initial conditions (72), were solved numerically; the results are shown in figure 14. The associated velocity profile development is shown in figures 15 and 16 with η and y, respectively, as independent variables. The profiles show spreading of the effected zone into the stream.

The steady second-order contribution to the wall shear stress is related to the y-derivative of the $\bar{u}_2$ profile, with the result evaluated at the wall. We define a shear

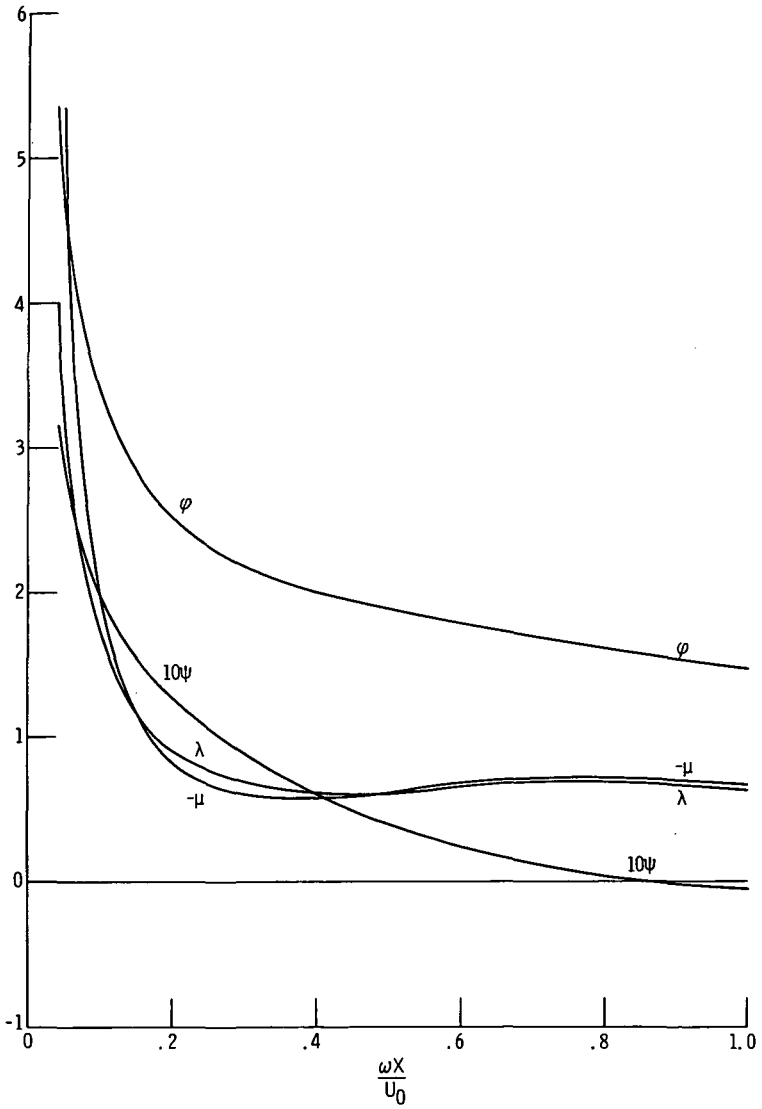

Figure 14. - Velocity profile form factors for time-independent second-order flow.

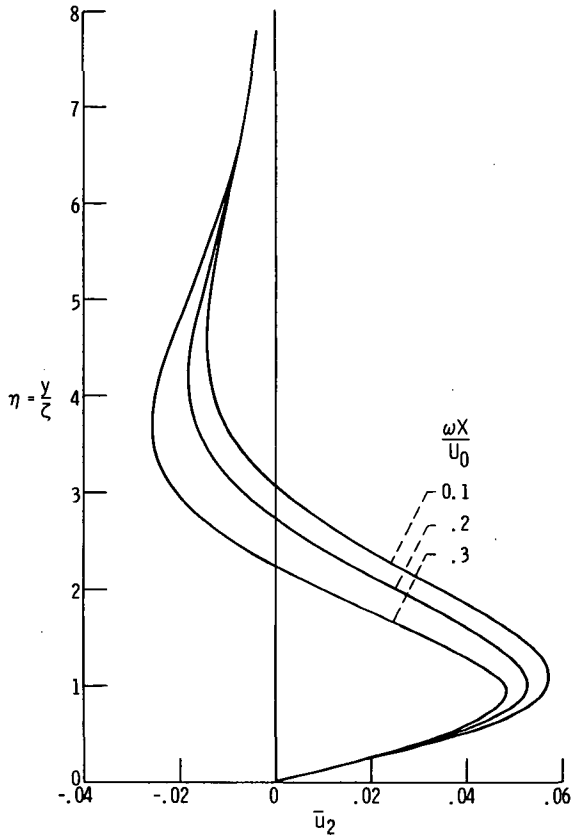

Figure 15. - Steady second-order velocity profiles (plotted against the similarity variable).

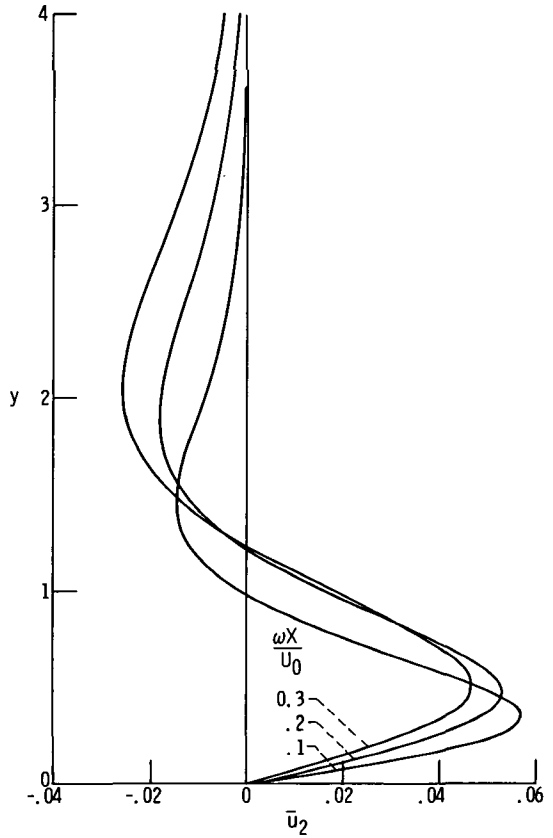

Figure 16. - Steady second-order velocity profiles (plotted against normal coordinate).

coefficient as the ratio of wall shear stress to the exact quasi-steady value, namely,

$$C_{\tau 2} = \frac{\left(\frac{\partial \bar{u}_2}{\partial y}\right)_{y=0}}{\left(\frac{\partial \bar{u}_{2Q}}{\partial y}\right)_{y=0}} \tag{74}$$

Values of the shear coefficient are compared with previous analytical results in figure 17.

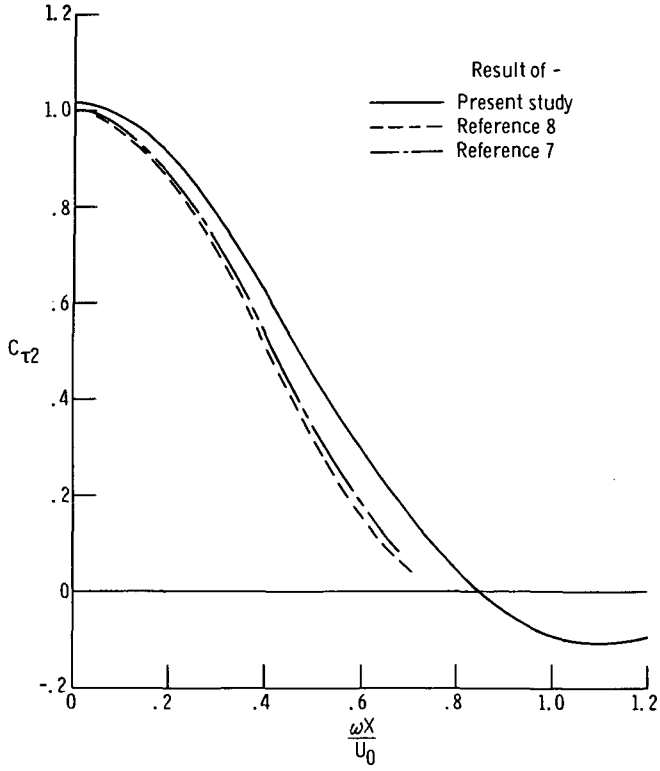

Figure 17. - Second-order wall shear stress coefficient.

THERMAL BOUNDARY LAYER ON A FLAT PLATE WITH AN OSCILLATING FREE STREAM

The thermal boundary layer is computed for the flat plate in a free stream with small harmonic velocity oscillations about a steady mean value. The free stream and

plate are at constant but different temperature levels. As a result of the velocity oscillations, the boundary-layer temperature performs small oscillations about the basic mean temperature distribution. Also, there is a small steady feedback of the oscillations on the mean heat transfer. We employ the integral method to obtain the thermal solution and utilize the previously derived velocity profiles.

Integral Relations

The boundary-layer heat transfer relies mainly on the steady temperature distribution due to the basic mean flow convection at constant plate-to-stream temperature difference. Temperature oscillations are of the first order (in ϵ) and are caused by the convective effect of the first-order velocity fluctuations. The steady second-order temperature is a result of the interaction between velocity and temperature oscillations, plus the convective effect of the steady mean flow correction $\bar{u}_2$. With these considerations, the dimensionless temperature is expanded as follows:

$$\theta = \theta_0(x,y) + \epsilon\theta_1(x,y)e^{i\omega t} + \epsilon^2\left[\bar{\theta}_2(x,y) + \tilde{\theta}_2(x,y,t)\right] + \mathcal{O}(\epsilon^3) \tag{75}$$

We substitute equation (75) into the thermal integral relation (14), nondimensionalize, and use the velocity profile expansion (16) to obtain the following thermal integral relations:

Order ϵ^0:

$$\frac{d}{dx}\int_0^\infty \frac{u_0}{k+1}\left(\theta_0^{k+1} - 1\right)dy = \begin{cases} -\dfrac{1}{Pr}\left(\dfrac{\partial\theta_0}{\partial y}\right)_{y=0} & k = 0 \\ -\dfrac{k}{Pr}\displaystyle\int_0^\infty \theta_0^{k-1}\left(\frac{\partial\theta_0}{\partial y}\right)^2 dy & k > 0 \end{cases} \tag{76}$$

Order ϵ^1:

$$\frac{d}{dx}\int_0^\infty \left[u_0\theta_0^k\theta_1 + \frac{u_1}{k+1}\left(\theta_0^{k+1} - 1\right)\right] dy = \begin{cases} -i\int_0^\infty \theta_1\, dy - \frac{1}{Pr}\left(\frac{\partial\theta_1}{\partial y}\right)_{y=0} & k = 0 \\ -1\int_0^\infty \theta_0^k\theta_1\, dy - \frac{k}{Pr}\int_0^\infty \left[2\theta_0^{k-1}\left(\frac{\partial\theta_0}{\partial y}\right)\left(\frac{\partial\theta_1}{\partial y}\right)\right. & \\ \left. + (k-1)\theta_0^{k-2}\theta_1\left(\frac{\partial\theta_0}{\partial y}\right)^2\right] dy & k > 0 \end{cases} \tag{77}$$

Order ϵ^2 (time-independent part):

$$\frac{d}{dx}\int_0^\infty \left[\frac{\bar{u}_2}{k+1}\left(\theta_0^{k+1} - 1\right) + \frac{1}{2}u_1^*\theta_1\theta_0^k + u_0\bar{\theta}_2\theta_0^k + \frac{k}{4}u_0\theta_1\theta_1^*\theta_0^{k-1}\right] dy$$

$$= \begin{cases} -\frac{1}{Pr}\left(\frac{\partial\bar{\theta}_2}{\partial y}\right)_{y=0} & k = 0 \\ -\frac{ik}{2}\int_0^\infty \theta_0^{k-1}\theta_1\theta_1^*\, dy - \frac{k}{Pr}\int_0^\infty \left[2\theta_0^{k-1}\left(\frac{\partial\theta_0}{\partial y}\right)\left(\frac{\partial\bar{\theta}_2}{\partial y}\right)\right. & \\ + \frac{1}{2}(k-1)\theta_0^{k-2}\frac{\partial\theta_0}{\partial y}\frac{\partial}{\partial y}\left(\theta_1\theta_1^*\right) + (k-1)\theta_0^{k-2}\bar{\theta}_2\left(\frac{\partial\theta_0}{\partial y}\right)^2 & \\ \left. + \frac{1}{2}\theta_0^{k-1}\frac{\partial\theta_1}{\partial y}\frac{\partial\theta_1^*}{\partial y} + \frac{(k-1)(k-2)}{4}\theta_0^{k-3}\theta_1\theta_1^*\left(\frac{\partial\theta_0}{\partial y}\right)\right] dy & k > 0 \end{cases} \tag{78}$$

where $Pr = \nu/\alpha_{th}$ is the Prandtl number.

We again use limiting-case solutions as guidelines to assume approximate temperature-profile forms. The detailed temperature distributions are then determined to satisfy the thermal integral equations (76) to (78).

Basic Mean Temperature

The basic mean temperature distribution is identified with the flat-plate boundary layer in a uniform free stream with zero plate temperature and unit stream temperature. This temperature distribution is the well-known similarity solution of the following boundary-value problem (cf. ref. 12):

$$\left.\begin{aligned} G'' + \frac{1}{2} Pr F_B G' = 0 \\ G(0) = 0 \\ G(\eta) \to 1 \quad \text{as} \quad \eta \to \infty \end{aligned}\right\} \tag{79}$$

The resulting solution is

$$G(\eta) = \frac{\int_0^{\eta} \left[F_B''(z)\right]^{Pr} dz}{\int_0^{\infty} \left[F_B''(z)\right]^{Pr} dz} \tag{80}$$

We obtain an approximation for the profile (80) by assuming the temperature distributions of the following form:

$$\theta_0 = 1 - e^{-\overline{A}\eta}(1 + \overline{B}\eta + \overline{C}\eta^2 + \overline{D}\eta^3) \tag{81}$$

The constants $\overline{A}$, $\overline{B}$, $\overline{C}$, and $\overline{D}$ are computed to satisfy the thermal integral relations (76) with $k = 0$, 1, 2, and 3. Upon changing variables $\left(\eta = y/\sqrt{x}\right)$ and introducing the function notation, there results

$$[F(3, 2) - F(3, 1)] + \frac{2}{Pr}\left(\overline{A} - \overline{B}\right) = 0 \tag{82}$$

$$[F(3,3) - F(3,3,2) - 2F(3,1) + 2F(3,2)] + \frac{4}{Pr}[F(4,4)] = 0 \tag{83}$$

$$[F(3,3,3,2) - F(3,3,3) - 3F(3,3,2) + F(3,3) + F(3,2) - 3F(3,1)]$$

$$+ \frac{12}{Pr}[F(4,4) - F(4,4,3)] = 0 \tag{84}$$

$$[F(3,3,3,3) - F(3,3,3,3,2) + 4F(3,3,3,2) - 4F(3,3,3) - 6F(3,3,2) + 6F(3,3) + 4F(3,2)$$

$$- 4F(3,1)] + \frac{24}{Pr}[F(4,4) - 2F(4,4,3) + F(4,4,3,3)] = 0 \tag{85}$$

where the following definitions are utilized:

$$[f_i] = \begin{bmatrix} 1 \\ 1 - u_0 \\ 1 - \theta_0 \\ d\theta_0/d\eta \end{bmatrix} \qquad [s_i] = \begin{bmatrix} 0 \\ A \\ \overline{A} \\ \overline{A} \end{bmatrix} \qquad [h_{im}] = \begin{bmatrix} 1 & 0 & 0 & 0 \\ 1 & B & C & D \\ 1 & \overline{B} & \overline{C} & \overline{D} \\ \overline{A} - \overline{B} & \overline{AB} - 2\overline{C} & \overline{AC} - 3\overline{D} & \overline{AD} \end{bmatrix} \tag{86}$$

The solution to the set of algebraic equations (82) to (85) is, for $Pr = 0.72$

$$\begin{bmatrix} \overline{A} \\ \overline{B} \\ \overline{C} \\ \overline{D} \end{bmatrix} = \begin{bmatrix} 1.665 \\ 1.367 \\ 0.6699 \\ 0.7161 \end{bmatrix} \tag{87}$$

The corresponding profile results are compared with the exact similarity solution in table II and also shown graphically in figure 18. In addition to the obvious agreement, we note the following comparison of slopes at the wall:

$$\left.\begin{aligned} \left(\frac{dG}{d\eta}\right)_{\eta=0} &= 0.2976 \\ \left(\frac{d\theta_0}{d\eta}\right)_{\eta=0} &= 0.2980 \end{aligned}\right\} \tag{88}$$

TABLE II. - COMPARISON OF ZEROTH-ORDER TEMPERATURE PROFILE APPROXIMATION WITH EXACT QUASI-STEADY SOLUTION

Similarity variable, $\eta = y/\zeta$	Exact solution	Approximate profile	Percent error
0.20	0.05913	0.06395	8.15
.40	.11822	.12670	7.18
.60	.17720	.18395	3.81
.80	.23590	.23746	.66
1.00	.29416	.28997	-1.43
1.20	0.35171	0.34333	-2.38
1.40	.40828	.39817	-2.48
1.60	.46355	.45412	-2.03
1.80	.51716	.51025	-1.34
2.00	.56876	.56539	-.59
2.20	0.61800	0.61838	0.06
2.40	.66455	.66828	.56
2.60	.70812	.71439	.89
2.80	.74845	.75626	1.04
3.00	.78536	.79370	1.06
3.20	0.81875	0.82672	0.97
3.40	.84858	.85549	.81
3.60	.87490	.88027	.61
3.80	.89781	.90140	.40
4.00	.91750	.91927	.19
4.20	0.93418	0.93424	0.01
4.40	.94812	.94670	-.15
4.60	.95962	.95699	-.27
4.80	.96896	.96544	-.36
5.00	.07645	.97235	-.42
5.20	0.98236	0.97795	-0.45
5.40	.98697	.98248	-.45
5.60	.99049	.98613	-.44
5.80	.99315	.98905	-.41
6.00	.99515	.99138	-.38
6.20	0.99662	0.99323	-0.34
6.40	.99769	.99470	-.30
6.60	.99845	.99586	-.26
6.80	.99899	.99678	-.22
7.00	.99936	.99749	-.19

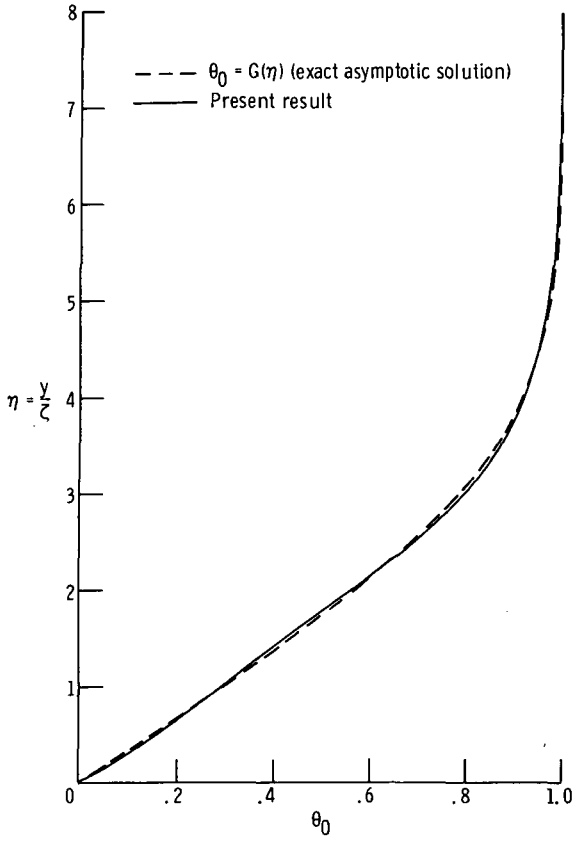

Figure 18. - Four-parameter profile approximation of the basic mean temperature distribution.

The wall slope is, of course, related to the basic mean heat transfer to the wall.

Temperature Oscillations

Oscillations in the temperature distribution are generated by the oscillating component of velocity. We compute these fluctuations by applying the integral method of analysis.

Quasi-steady temperature. - We first consider the quasi-steady effect of low-frequency velocity fluctuations, that is, the steady temperature distribution with instantaneous uniform stream velocity $U_0(1 + \epsilon e^{i\omega t})$, namely,

$$\theta_Q = G\left(\frac{y}{\sqrt{x}}\sqrt{1 + \epsilon e^{i\omega t}}\right) \tag{89}$$

Now, the temperature distribution (89) is expanded in a Taylor series for small free-stream perturbations and the first-order quasi-steady temperature is readily identified as the following:

$$\theta_{1Q} = \frac{1}{2}\eta G'(\eta) \tag{90}$$

This profile (for $Pr = 0.72$) is indicated by the dashed line in figure 19.

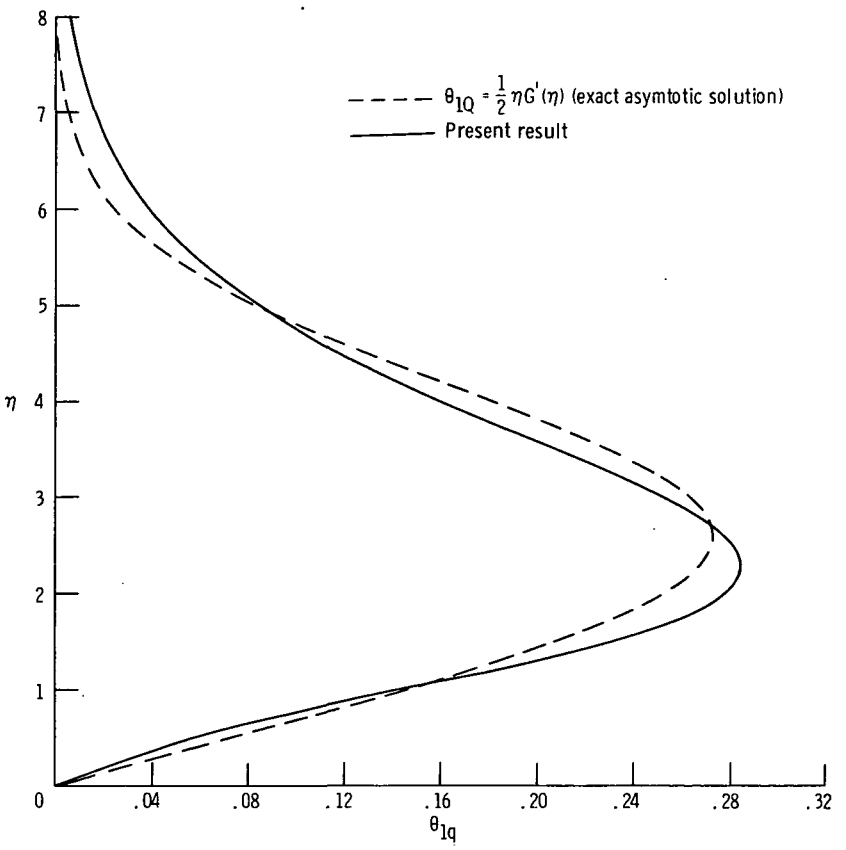

Figure 19. - First-order quasi-steady temperature distribution.

An approximation for θ_{1Q} is obtained with the integral method by assuming the profile form

$$\theta_{1q} = e^{-\bar{a}\eta}(\bar{b}\eta + \bar{c}\eta^2 + \bar{d}\eta^3) \tag{91}$$

We introduce the following definitions:

$$[f_i] = \begin{bmatrix} 1 \\ 1 - u_0 \\ 1 - \theta_0 \\ d\theta_0/d\eta \\ 1 - u_{1q} \\ \theta_{1q} \\ d\theta_{1q}/d\eta \end{bmatrix} \quad [s_i] = \begin{bmatrix} 0 \\ A \\ \bar{A} \\ \bar{A} \\ a \\ \bar{a} \\ \bar{a} \end{bmatrix} \quad [h_{im}] = \begin{bmatrix} 1 & 0 & 0 & 0 \\ 1 & B & C & D \\ 1 & \bar{B} & \bar{C} & \bar{D} \\ \bar{A} - \bar{B} & \overline{AB} - 2\bar{C} & \overline{AC} - 3\bar{D} & \overline{AD} \\ 1 & b & c & d \\ 0 & \bar{b} & \bar{c} & \bar{d} \\ \bar{b} & 2\bar{c} - \overline{ab} & 3\bar{d} - \overline{ac} & \overline{ad} \end{bmatrix} \tag{92}$$

Then, following the usual procedure, the thermal integral relations (77) for $k = 0, 1, 2,$ and 3 are reduced, for the quasi-steady case, to the following:

$$[F(6,1) - F(6,2)] + [F(5,3) - F(3,1)] + \frac{2\bar{b}}{Pr} = 0 \tag{93}$$

$$2[F(6,1) - F(6,2) - F(6,3) + F(6,3,2)] + [F(3,3) - F(5,3,3) - 2F(3,1) + 2F(5,3)] + \frac{8}{Pr}[F(7,4)] = 0 \tag{94}$$

$$3[F(6,1) - 2F(6,3) - F(6,2) + F(6,3,3) + 2F(6,3,2) - F(6,3,3,2)] + \frac{12}{Pr}[F(6,4,4) + 2F(7,4) - 2F(7,4,3)] - [F(3,3,3) - 3F(3,3) + 3F(3,1) - F(5,3,3,3) + 3F(5,3,3) - 3F(5,3)] = 0 \tag{95}$$

$$4[F(6,1) - 3F(6,3) + 3F(6,3,3) - F(6,3,3,3) - F(6,2) + 3F(6,3,2) - 3F(6,3,3,2) + F(6,3,3,3,2)] + [F(3,3,3,3) - 4F(3,3,3) + 6F(3,3) - 4F(3,1) - F(5,3,3,3,3) + 4F(5,3,3,3) - 6F(5,3,3) + 4F(5,3)] + \frac{48}{Pr}[F(7,4) - 2F(7,4,3) + F(7,4,3,3) + F(6,4,4) - F(6,4,4,3)] = 0 \tag{96}$$

The solution of the profile constants from these equations gives

$$\begin{bmatrix} \bar{a} \\ \bar{b} \\ \bar{c} \\ \bar{d} \end{bmatrix} = \begin{bmatrix} 1.31812 \\ 0.14310 \\ -0.11436 \\ 0.50646 \end{bmatrix} \tag{97}$$

The resulting quasi-steady profile approximation is shown in figure 19. We also note here the corresponding wall slopes for the exact limiting-case solution and approximate result:

$$\left.\begin{aligned} \left(\frac{d\theta_{1Q}}{d\eta}\right)_{\eta=0} &= 0.1488 \\ \left(\frac{d\theta_{1q}}{d\eta}\right)_{\eta=0} &= 0.1431 \end{aligned}\right\} \tag{98}$$

Profile parameters. - The general fluctuating temperature profile is assumed to be of the following form:

$$\theta_1 = e^{-\bar{\alpha}y}(\bar{\beta}y + \bar{\gamma}y^2 + \bar{\delta}y^3) \tag{99}$$

The coefficients ($\bar{\alpha}$, $\bar{\beta}$, $\bar{\gamma}$, and $\bar{\delta}$) are complex functions of the variable $\zeta = \sqrt{\omega X/U_0}$. Thus, the temperature oscillations have components in phase and out of phase with the free-stream velocity fluctuations.

The thermal integral relations (77) reduce to a set of ordinary differential equations when the profile (99) is introduced. The details of the differential equations are given in appendix E and the equations are of the form

$$P_{i1}\frac{d\bar{\alpha}}{d\zeta} + P_{i2}\frac{d\bar{\beta}}{d\zeta} + P_{i3}\frac{d\bar{\gamma}}{d\zeta} + P_{i4}\frac{d\bar{\delta}}{d\zeta} = R_i \qquad i = 1,\ 2,\ 3,\ 4 \tag{100}$$

Of course, the real initial values for equation (100) are the quasi-steady limits, namely,

$$\begin{bmatrix} \bar{\alpha}_r \\ \bar{\beta}_r \\ \bar{\gamma}_r \\ \bar{\delta}_r \end{bmatrix} \sim \begin{bmatrix} \bar{a}/\zeta \\ \bar{b}/\zeta \\ \bar{c}/\zeta^2 \\ d/\zeta^3 \end{bmatrix} \quad \text{as } \zeta \to 0 \tag{101}$$

We obtain the imaginary initial values by introducing an expansion of the identical form as equations (59). Substituting the expansions into equation (100) and solving the resulting algebraic equations by the method of appendix D then yields

$$\begin{bmatrix} \bar{\alpha}_i \\ \bar{\beta}_i \\ \bar{\gamma}_i \\ \bar{\delta}_i \end{bmatrix} \sim \begin{bmatrix} 0.06196\ \zeta \\ -0.02901\ \zeta \\ -0.08295 \\ 0.06885/\zeta \end{bmatrix} \quad \text{as } \zeta \to 0 \tag{102}$$

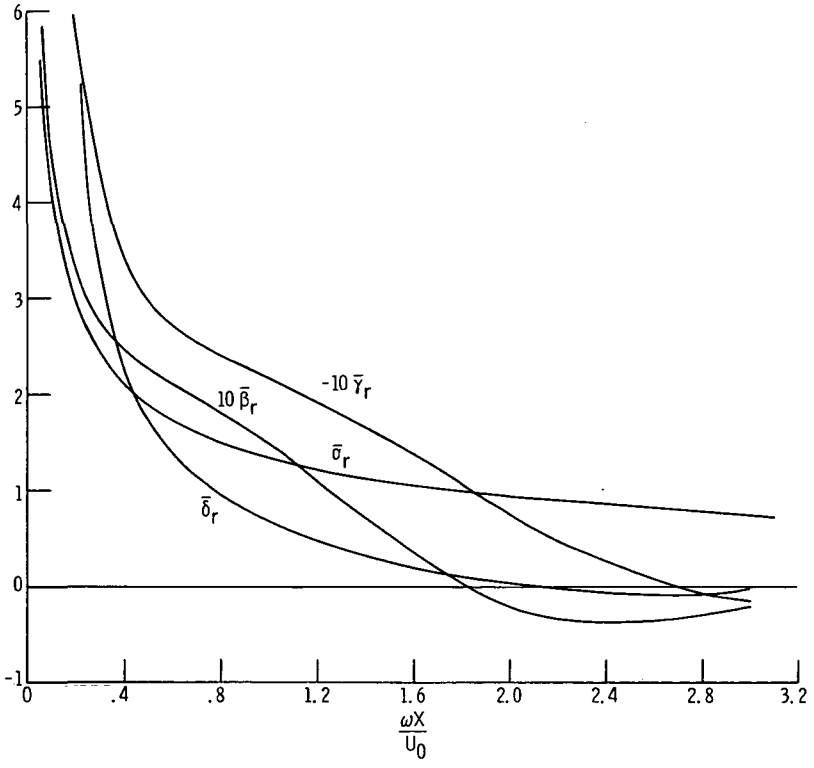

Figure 20. - Real parts of first-order temperature profile form parameters.

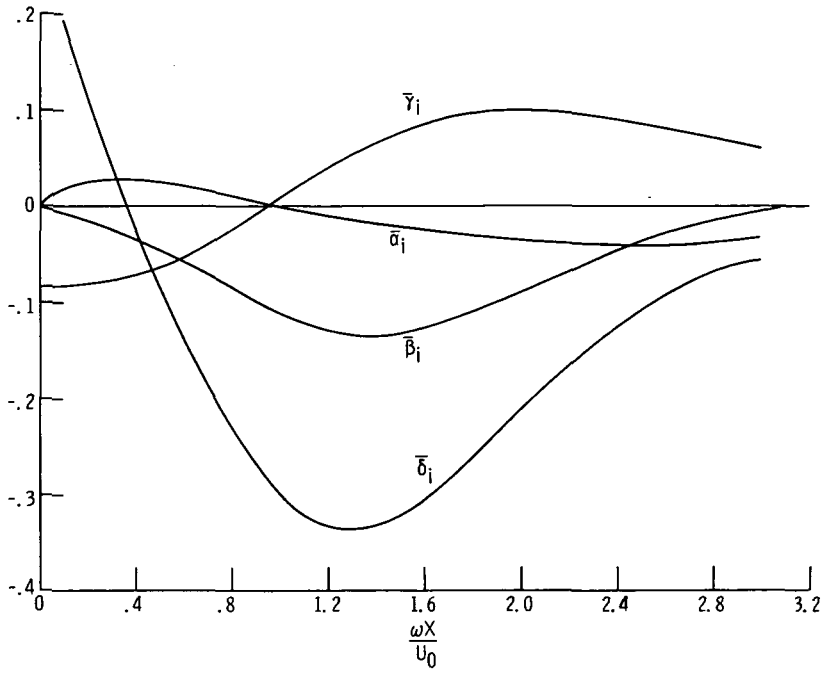

Figure 21. - Imaginary parts of first-order temperature profile form parameters.

Numerical solution of equations (100) with initial values (101) and (102) gives the profile form parameters shown graphically in figures 20 and 21.

Temperature profile results. - The in-phase and out-of-phase temperature profiles are plotted against η in figures 22 and 23 for small values of $\zeta = \sqrt{\omega X/U_0}$. We see that as the profiles develop, the peak value increases but remains at approximately the same value of η.

The profile development for large values of ζ is shown in figures 24 and 25 with the independent variable y. We note the spreading of the effected layer into the free stream and ultimately a reduction of both components for very large ζ.

We define the engineering heat-transfer quantities in the usual manner. The heat flux at the wall is

$$Q_w = -\kappa \left(\frac{\partial T}{\partial Y}\right)_{Y=0} \tag{103}$$

The flux is related to the Nusselt number Nu_X as follows:

$$Q_w = \frac{\kappa}{X} Nu_X (T_w - T_\infty) \tag{104}$$

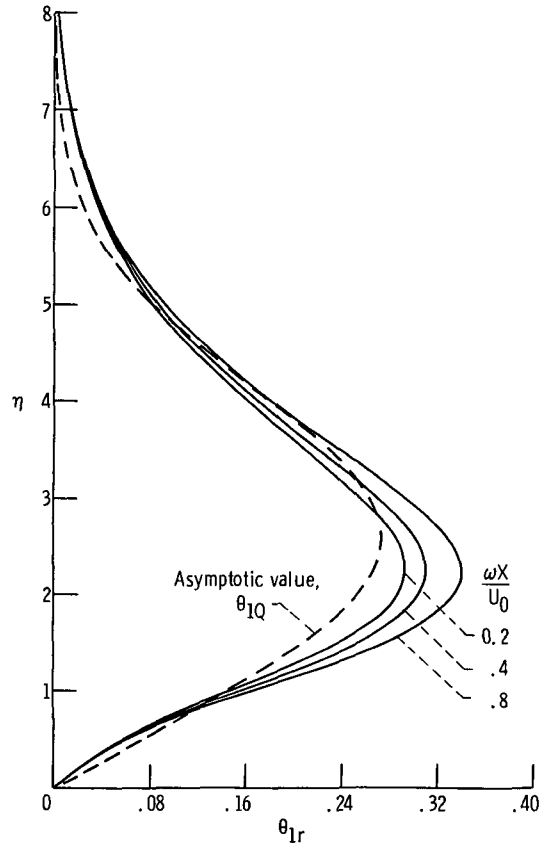

Figure 22. - In-phase component of first-order temperature fluctuations for small values of ζ.

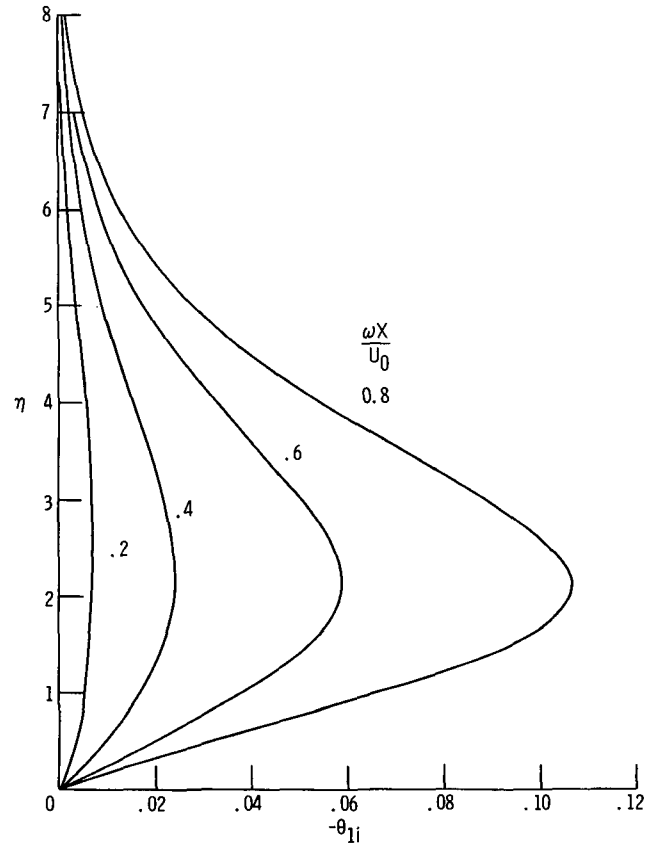

Figure 23. - Out-of-phase component of first-order temperature fluctuations for small values of ζ.

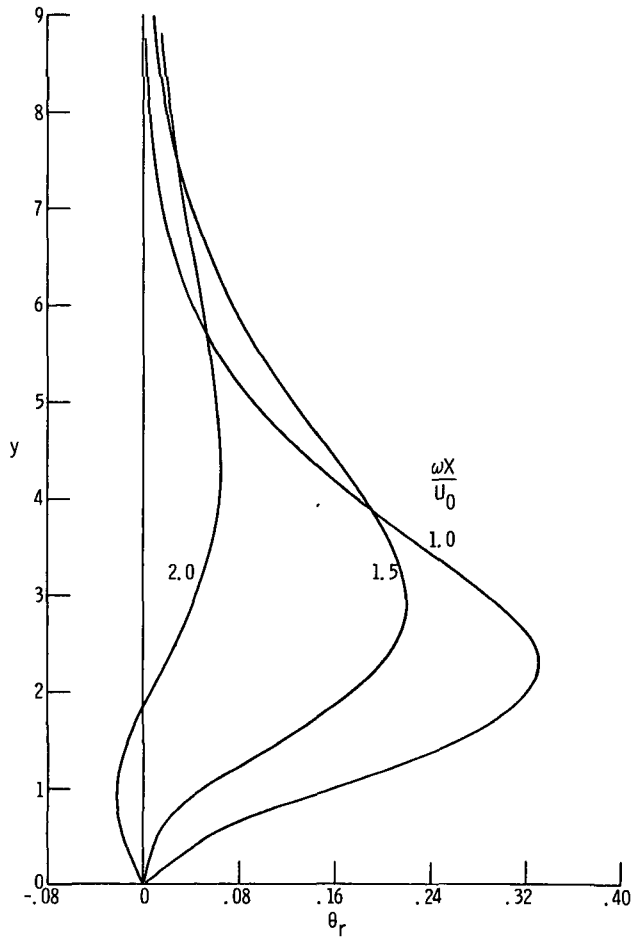

Figure 24. - In-phase component of first-order temperature fluctuations for large values of ζ.

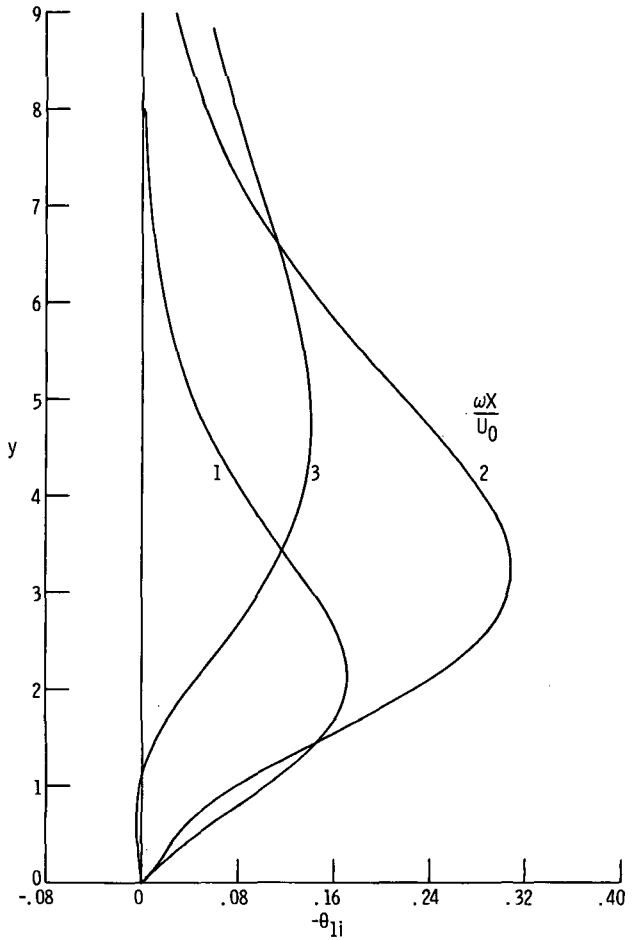

Figure 25. - Out-of-phase component of first-order temperature fluctuations for large values of ζ.

We consider here the ratio of the first-order to the mean-flow Nusselt number and define this heat-flux ratio as follows:

$$C_{Q1} = \frac{\left(\frac{\partial \theta_1}{\partial y}\right)_{y=0}}{\left(\frac{\partial \theta_0}{\partial y}\right)_{y=0}} \tag{105}$$

The real and imaginary parts of the heat-flux ratio are shown in figure 26.

The first-order heat transfer is oscillatory in nature and thus gives no net contribution to the overall heat transfer in the time-average sense.

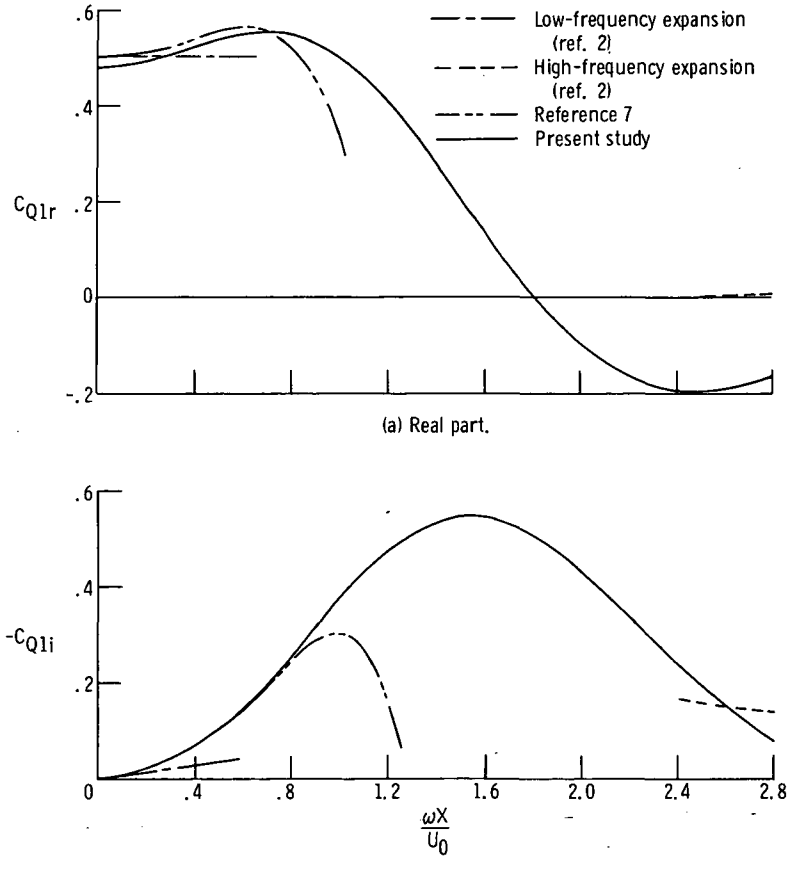

Figure 26. - First-order wall heat-flux ratio.

Effect of Oscillations on the Time-Average Temperature

We now compute the effect of velocity and temperature oscillations on the time-average temperature distribution. The steady mean temperature correction is a result of the interaction between the first-order temperature and velocity oscillations plus the thermal convection due to the second-order mean flow.

Quasi-steady temperature. - The second-order quasi-steady temperature distribution (limiting case for low-frequency fluctuations) is computed directly from the small perturbation expansion of equation (89). The result is

$$\bar{\theta}_{2Q} = \frac{\eta}{16}(\eta G'' - G') \tag{106}$$

This profile is given in figure 27.

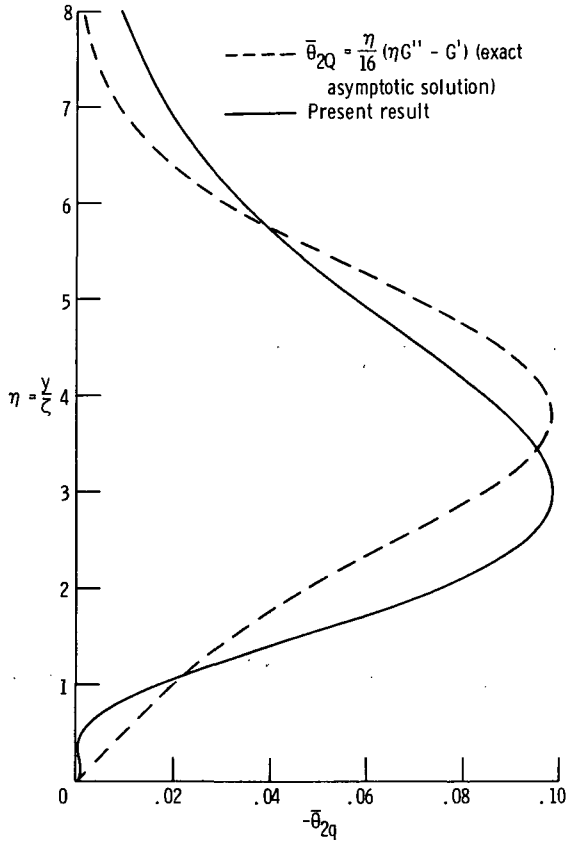

Figure 27. - Second-order quasi-steady temperature profile.

The quasi-steady approximation profile is assumed to have the following form:

$$\bar{\theta}_{2q} = e^{-\bar{p}\eta}(\bar{q}\eta + \bar{r}\eta^2 + \bar{s}\eta^3) \tag{107}$$

We now introduce the arrays

$$[f_i] = \begin{bmatrix} 1 \\ 1 - u_0 \\ 1 - u_1 \\ \bar{u}_2 \\ 1 - \theta_0 \\ \theta_1 \\ \theta_2 \\ d\theta_0/d\eta \\ d\theta_1/d\eta \\ d\bar{\theta}_2/d\eta \end{bmatrix} \quad [s_i] = \begin{bmatrix} 0 \\ A \\ a \\ p \\ \bar{A} \\ \bar{a} \\ \bar{p} \\ \bar{A} \\ \bar{a} \\ \bar{p} \end{bmatrix} \quad [h_{im}] = \begin{bmatrix} 1 & 0 & 0 & 0 \\ 1 & B & C & D \\ 1 & b & c & d \\ 0 & q & r & s \\ 1 & \bar{B} & \bar{C} & \bar{D} \\ 0 & \bar{b} & \bar{c} & \bar{d} \\ 0 & \bar{q} & \bar{r} & \bar{s} \\ \bar{A} - \bar{B} & \overline{AB} - 2\bar{C} & \overline{AC} - 3\bar{D} & \overline{AD} \\ \bar{b} & 2\bar{c} - \overline{ab} & 3\bar{d} - \overline{ac} & -\overline{ad} \\ \bar{q} & 2\bar{r} - \overline{pq} & 3\bar{c} - \overline{pr} & -\overline{ps} \end{bmatrix} \tag{108}$$

Then, following the usual procedure for similarity profiles, we reduce the thermal integral relations (78) for k = 0, 1, 2, and 3 to the following:

$$[F(6,1) - F(6,3)] + 2[F(7,1) - F(7,2)] - 2[F(5,4)] + \frac{4}{Pr}\bar{q} = 0 \tag{109}$$

$$[F(6,6) - F(6,6,2)] + 4[F(7,1) - F(7,2) - F(7,5) + F(7,5,2)] + 2[F(6,1) - F(6,5) - F(6,3) + F(6,5,3)] + 2[F(5,5,4) - 2F(5,4)] + \frac{4}{Pr}[4F(10,8) + F(9,9)] = 0 \tag{110}$$

$$3[F(6,6) - F(6,6,2) - F(6,6,5) + F(6,6,5,2)] + 6[F(7,1) - F(7,2) - 2F(7,5) + 2F(7,5,2)$$

$$+ F(7,5,5) - F(7,5,5,2)] + 3[F(6,1) - 2F(6,5) - F(6,3) + 2F(6,5,3) + F(6,5,5)$$

$$- F(6,5,5,3)] - 2[F(5,5,5,4) - 3F(5,5,4) + 3F(5,4)] + \frac{12}{Pr}[4F(10,8)$$

$$- 4F(10,8,5) + 2F(9,8,6) + 2F(8,8,7) + F(9,9) - F(9,9,5)] = 0 \qquad (111)$$

$$3[F(6,6) - F(6,6,2) - 2F(6,6,5) + 2F(6,6,5,2) + F(6,6,5,5) - F(6,6,5,5,2)] + 4[F(7,1)$$

$$-F(7,2) - 3F(7,5) + 3F(7,5,2) + 3F(7,5,5) - 3F(7,5,5,2) - F(7,5,5,5)$$

$$+ F(7,5,5,5,2)] + 2[F(6,1) - 3F(6,5) - F(6,3) + 3F(6,5,3) + 3F(6,5,5)$$

$$- 3F(6,5,5,3) - F(6,5,5,5) + F(6,5,5,5,3)] - [4F(5,4) - 6F(5,5,4)$$

$$+ 4F(5,5,5,4) - F(5,5,5,5,4)] + \frac{12}{Pr}[4F(10,8) - 8F(10,8,5) + 4F(10,8,5,5)$$

$$+ 4F(9,8,6) - 4F(9,8,6,5) + 4F(8,8,7) - 4F(8,8,7,5) + F(9,9) - 2F(9,9,5)$$

$$+ F(9,9,5,5) + F(8,8,6,6)] = 0 \qquad (112)$$

The preceding equations admit the following solution:

$$\begin{bmatrix} \bar{p} \\ \bar{q} \\ \bar{r} \\ \bar{s} \end{bmatrix} = \begin{bmatrix} 1.08776 \\ -0.018378 \\ 0.091511 \\ -0.12387 \end{bmatrix} \qquad (113)$$

The profile corresponding to the result (113) is shown in figure 27. The approximation gives the general shape desired, and the peak values agree very well in magnitude and reasonably well in location.

It is of interest that the slope of the approximate profile at the wall compares with the quasi-steady limit value as follows:

$$\left.\begin{aligned}\left(\frac{d\bar{\theta}_{2Q}}{d\eta}\right)_{\eta=0} &= -0.01860\\ \left(\frac{d\bar{\theta}_{2q}}{d\eta}\right)_{\eta=0} &= -0.01838\end{aligned}\right\} \tag{114}$$

These slopes agree even though the curves have different shapes near the wall. We investigate this effect by assuming profiles with other slopes at the wall (i.e., pick $\bar{q}$ in eq. (107)). The remaining three shape factors in equation (107) are determined to satisfy equations (110) to (112). The profiles considered are

$$\left.\begin{aligned}\bar{\theta}_{2q}^{(-)} &= e^{-1.0761\eta}(-0.10\,\eta + 0.07370\,\eta^2 - 0.1154\,\eta^3)\\ \bar{\theta}_{2q}^{(+)} &= e^{-1.0639\eta}(-0.30\,\eta + 0.07024\,\eta^2 - 0.1084\,\eta^3)\end{aligned}\right\} \tag{115}$$

The behavior of the various profiles is compared in figure 28. The profile value for $\eta > 1$ is completely determined by the coefficients $\bar{p}$, $\bar{r}$, and $\bar{s}$. Thus, the value of $\bar{q}$ which satisfies equation (109) is that which causes $\bar{\theta}_{2q}$ to satisfy the heat-flux integral near the wall.

Profile factors. - The steady second-order temperature profile, which applies for all frequency values, has the form

$$\bar{\theta}_2 = e^{-\bar{\varphi}y}(\bar{\psi}y + \bar{\mu}y^2 + \bar{\lambda}y^3) \tag{116}$$

We compute the profile form factors in the usual manner by the integral method. The thermal integral relations (78) reduce to differential equations of the following form:

$$P_{i1}\frac{d\bar{\varphi}}{d\zeta} + P_{i2}\frac{d\bar{\psi}}{d\zeta} + P_{i3}\frac{d\bar{\mu}}{d\zeta} + P_{i4}\frac{d\bar{\lambda}}{d\zeta} = R_i \qquad i = 1,\ 2,\ 3,\ 4 \tag{117}$$

The coefficients P_{ij} and R_i are listed in appendix E.

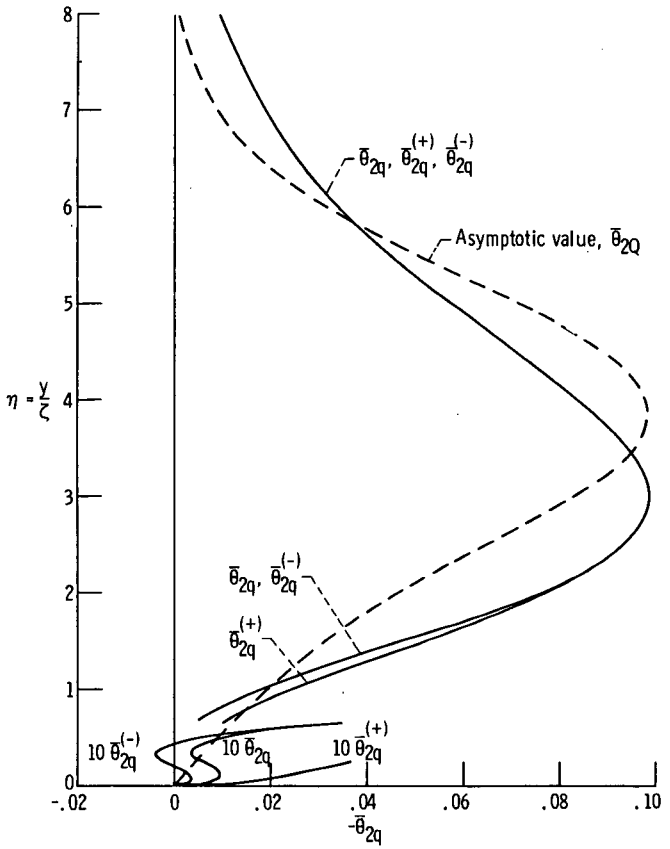

Figure 28. - Behavior of four-parameter second-order quasi-steady temperature profile approximations.

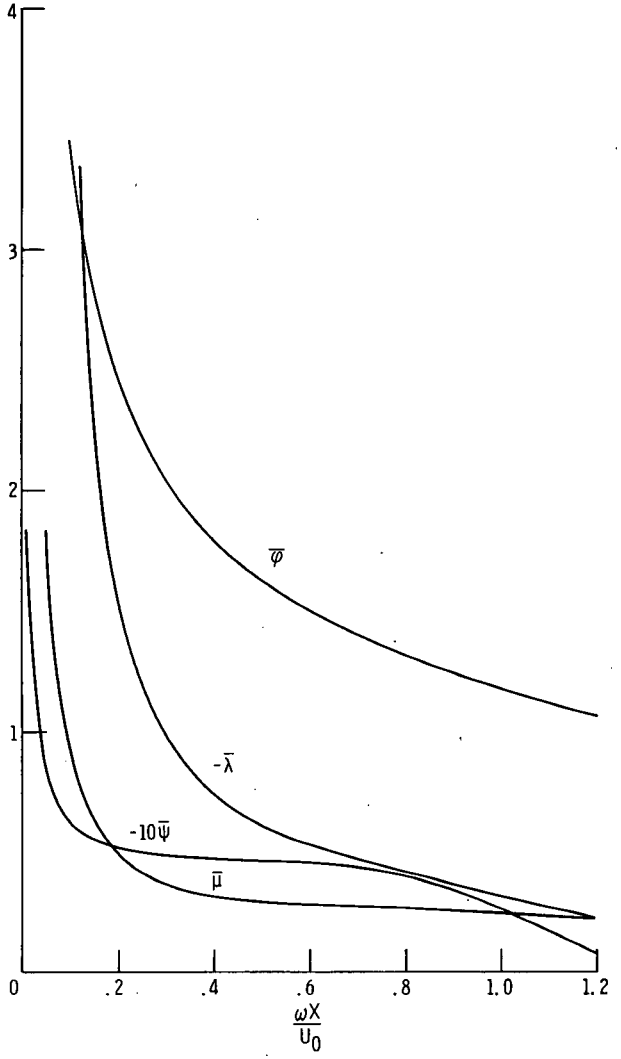

Figure 29. - Time-independent second-order temperature profile form factors.

The initial values of the profile factors are obtained from the quasi-steady distribution, that is,

$$\begin{bmatrix} \bar{\varphi} \\ \bar{\psi} \\ \bar{\mu} \\ \bar{\lambda} \end{bmatrix} \sim \begin{bmatrix} \bar{p}/\zeta \\ \bar{q}/\zeta \\ \bar{r}/\zeta^2 \\ \bar{s}/\zeta^3 \end{bmatrix} \quad \text{as } \zeta \to 0 \tag{118}$$

The numerical solution of this initial-value problem, equations (117) and (118), is presented graphically in figure 29.

Temperature distribution. - The development of the steady second-order temperature profiles is shown in figures 30 and 31. We see that the initial departure from

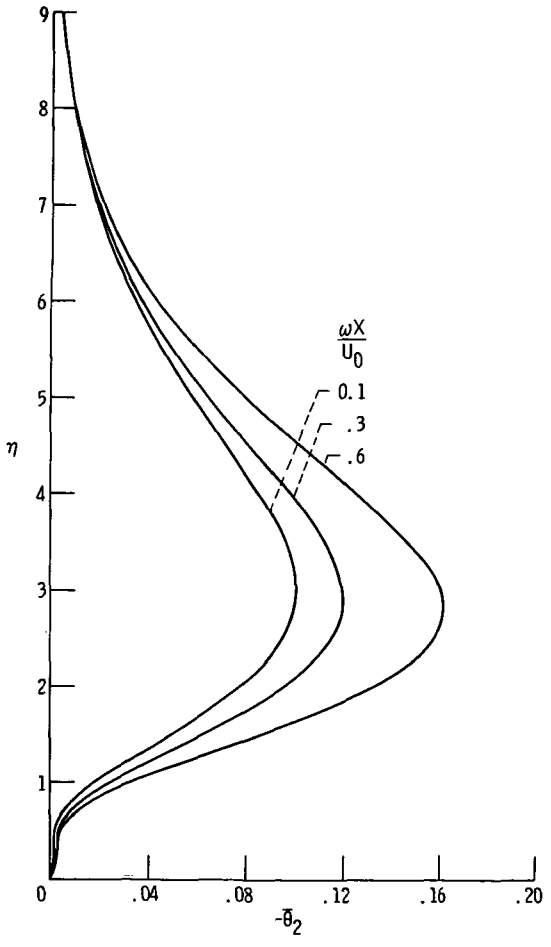

Figure 30. - Steady second-order temperature profiles for small values of ζ.

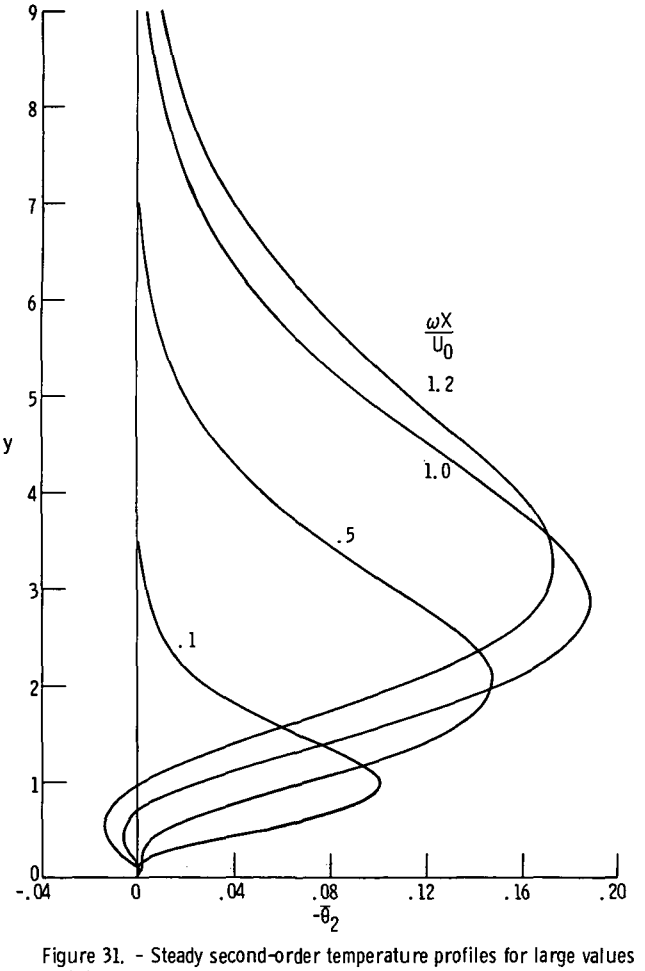

Figure 31. - Steady second-order temperature profiles for large values of ζ.

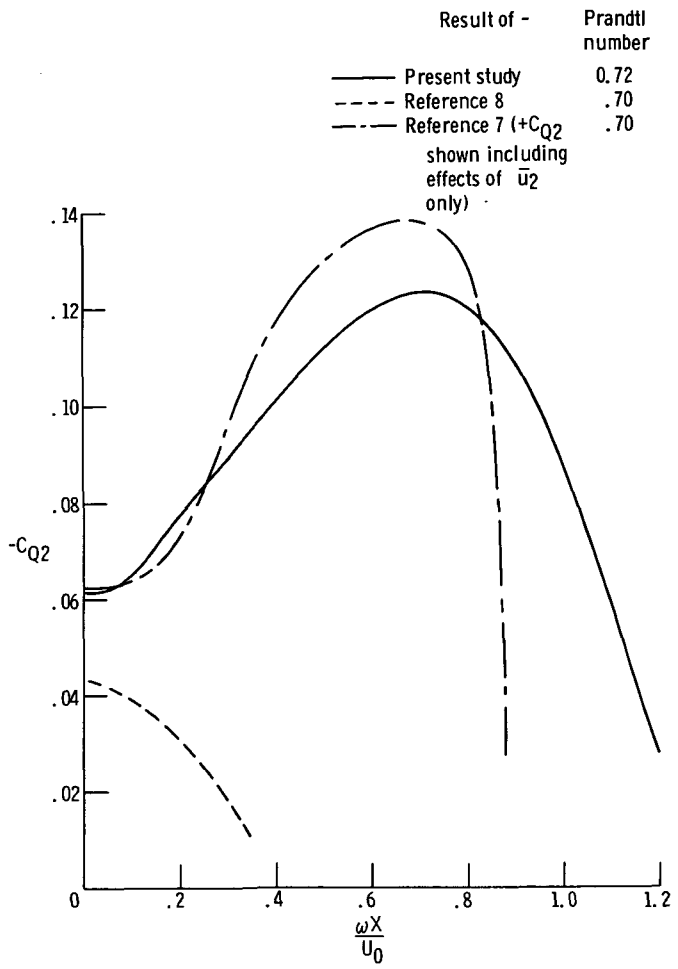

Figure 32. - Steady second-order heat-flux ratio.

quasi-steady behavior is to increase the maximum value, with that maximum occurring at about the same value of η (fig. 30). The layer then spreads into the stream (fig. 31) and ultimately diminishes in value.

A second-order heat-flux ratio is defined as follows:

$$C_{Q2} = \frac{\left(\frac{\partial \bar{\theta}_2}{\partial y}\right)_{y=0}}{\left(\frac{\partial \theta_0}{\partial y}\right)_{y=0}} \tag{119}$$

Values of this ratio are compared with results of other analytical investigations in figure 32. All previous work is asymptotically valid for small $\omega X/U_0$. Thus, the trend

of the Gersten result is confirmed over the full range of frequency. The Nickerson data are for the heat-transfer contribution of the second-order steady velocity and neglect the oscillating velocity-temperature interaction.

We use the preceding heat-transfer results, together with equation (103), to express the mean rate of heat transfer to the plate. The result for $Pr = 0.72$ is

$$\frac{(Q_w)_{mean}}{\kappa(T_w - T_\infty)\sqrt{U_0/\nu X}} = 0.298\left(1 + \epsilon^2 C_{Q2}\right) \tag{120}$$

The corresponding values of C_{Q2} are shown in figure 32. Since C_{Q2} is negative, the effect of flow oscillations is a small reduction in the mean heat transfer to the plate.

SUMMARY AND CONCLUSIONS

The general integral method of analysis was developed for the unsteady thermal boundary layer. The development was based on the flat-plate geometry with time-dependent free-stream velocity. The stream and plate were taken to be at constant but different temperature levels.

A system of integral relations was derived based on the momentum and thermal energy equations. The flow integral relations are velocity-weighted averages of the momentum equation. The thermal integral relations are temperature-weighted averages of the thermal energy equation.

The integral method then consists of the following: Obtain asymptotic solutions for limiting cases of the flow and heat transfer under consideration. Assume velocity and temperature profile forms with sufficient generality to include the asymptotic solutions. Determine profile form factors to satisfy the appropriate integral relations.

A detailed analysis was performed for the special case of a free stream with small harmonic velocity oscillations about a steady mean value. The velocity was found to consist of a steady mean flow corresponding to the Blasius flow, first-order velocity oscillations, and a second-order correction to the mean flow due to feedback of the oscillations. The basic mean temperature distribution was found to be the well-known flat-plate steady-boundary-layer result. First-order temperature oscillations were generated by the velocity oscillations.

The second-order steady temperature correction was caused by the velocity-temperature oscillation interaction plus the steady second-order flow convection effect. Oscillations were found to reduce the mean heat transfer to the plate. The amount of decrease is represented by a single coefficient, which is presented graphically. Flow

and heat-transfer results were found to adequately span the asymptotic limiting-case solutions.

Although the analysis herein was specialized for certain geometry, free stream, and boundary conditions, the basic method could be applied to many other configurations of interest.

Lewis Research Center,
National Aeronautics and Space Administration,
Cleveland, Ohio, August 4, 1972,
503-10.

APPENDIX A

SYMBOLS

A	Blasius profile approximation form factor
$\overline{A}$	zeroth-order temperature profile form factor
a	first-order quasi-steady velocity profile factor
$\overline{a}$	first-order quasi-steady temperature profile factor
$\tilde{a}$	imaginary coefficient in α expansion, eq. (59)
B	Blasius profile approximation form factor
$\overline{B}$	zeroth-order temperature profile form factor
b	first-order quasi-steady velocity profile factor
$\overline{b}$	first-order quasi-steady temperature profile factor
$\tilde{b}$	imaginary coefficient in β expansion, eq. (59)
C	Blasius profile approximation form factor
$\overline{C}$	zeroth-order temperature profile form factor
C_0	constant, eq. (36)
C_Q	heat-flux ratio
$C_{\tau 1}$	first-order wall shear stress coefficient, eq. (62)
$C_{\tau 2}$	second-order wall shear stress coefficient, eq. (74)
c	first-order quasi-steady velocity profile factor
$\overline{c}$	first-order quasi-steady temperature profile factor
$\tilde{c}$	imaginary coefficient in γ expansion, eq. (59)
D	Blasius profile approximation form factor
$\overline{D}$	zeroth-order temperature profile form factor
d	first-order quasi-steady velocity profile factor
$\overline{d}$	first-order quasi-steady temperature profile factor
$\tilde{d}$	imaginary coefficient in δ expansion, eq. (59)
F_B	Blasius flow dimensionless stream function
f_i	profile summation function
G	zeroth-order flat-plate temperature profile, eq. (80)

g_i	functions, appendix D
H_{im}	profile approximation matrix
h_{im}	profile approximation matrix
I_i	integrals, appendixes B and C
k	nonnegative integer
k_i	Runge-Kutta functions, appendix F
l_i	Runge-Kutta functions, appendix F
m_i	Runge-Kutta functions, appendix F
Nu_x	Nusselt number
n_i	Runge-Kutta functions, appendix F
P	pressure
P_{ij}	coefficients in differential equations
Pr	Prandtl number, ν/α_{th}
p	second-order quasi-steady velocity profile factor
$\overline{p}$	second-order quasi-steady temperature profile factor
Q_w	heat flux at wall
q	second-order quasi-steady velocity profile factor
$\overline{q}$	second-order quasi-steady temperature profile factor
R_i	terms in differential equations
r	second-order quasi-steady velocity profile factor
$\overline{r}$	second-order quasi-steady temperature profile factor
S_i	attenuation matrix
s	second-order quasi-steady velocity profile factor
$\overline{s}$	second-order quasi-steady temperature profile factor
s_i	attenuation matrix
T	temperature
t	time
U	velocity component parallel to the body
U_0	mean value of free-stream velocity
u	dimensionless velocity component parallel to the body, U/U_0

$\bar{u}_2$	time-independent part of second-order velocity
$\tilde{u}_2$	time-dependent part of second-order velocity
V	velocity component normal to the body
X	coordinate along the body
x	dimensionless coordinate along the body, $\omega X/U_0$
Y	coordinate normal to the body
y	dimensionless coordinate normal to the body, $\sqrt{\frac{\omega}{\nu}}\ Y$
Z	dummy variable, eq. (36)
α	first-order velocity profile form function
$\bar{\alpha}$	first-order temperature profile form function
α_{th}	thermal diffusivity
β	first-order velocity profile form function
$\bar{\beta}$	first-order temperature profile form function
γ	first-order velocity profile form function
$\bar{\gamma}$	first-order temperature profile form function
Δ	increment in Runge-Kutta integration formulas, appendix F
δ	first-order velocity profile form function
$\bar{\delta}$	first-order temperature profile form function
ϵ	amplitude of harmonic free-stream velocity fluctuation
ζ	stretched coordinate, $\sqrt{x}$
η	similarity variable, y/ζ
θ	dimensionless temperature, $(T - T_w)/(T_\infty - T_w)$
κ	thermal conductivity
λ	second-order velocity profile factor
$\bar{\lambda}$	second-order temperature profile factor
μ	second-order velocity profile factor
$\bar{\mu}$	second-order temperature profile factor
ν	kinematic viscosity
π	differential function, eq. (57)

ρ	density
Φ_τ	phase angle of first-order wall shear stress coefficient
φ	second-order velocity profile form function
$\overline{\varphi}$	second-order temperature profile form function
ψ	second-order velocity profile form functions
$\overline{\psi}$	second-order temperature profile form functions
Ω	function, eq. (25)
ω	frequency of harmonic free-stream fluctuations

Subscripts:

B	Blasius flow value
i	imaginary part
Q	quasi-steady expansion value
q	quasi-steady approximation value
r	real part
S	Stokes flow value
w	value at plate surface
0	zeroth-order (ϵ^0) value
1	first-order (ϵ^1) value
2	second-order (ϵ^2) value
∞	free-stream value

Special symbols:

F(I,J,K,L)	integration summation function, eq. (35)
G(I,J,K,L)	integration summation function, eq. (E2)
$\mathcal{O}$	order symbol
Re{ }	real part
Im{ }	imaginary part
Z*	denotes complex conjugate of Z, or prescribed Z in appendix D
$\lvert Z \rvert$	denotes magnitude of Z
$\overline{\theta}_{2q}^{(+)}, \overline{\theta}_{2q}^{(-)}$	temperature profiles, eq. (115)

APPENDIX B

DERIVATION OF THE FLOW INTEGRAL RELATIONS

The X-momentum equation (2) is multiplied by a nonnegative power of the local axial velocity U^k and integrated in the direction normal to the plate from the surface to the free stream. The result is

$$\int_0^\infty U^k \frac{\partial U}{\partial t}\,dY + \int_0^\infty \left(U^{k+1}\frac{\partial U}{\partial X} + U^k V \frac{\partial U}{\partial Y}\right)dY$$

$$= \int_0^\infty U^k \frac{\partial U_\infty}{\partial t}\,dY + \nu \int_0^\infty U^k \frac{\partial^2 U}{\partial Y^2}\,dY \qquad \text{(B1)}$$

First, consider the following integral:

$$I_1 = \int_0^\infty V U^k \frac{\partial U}{\partial Y}\,dY \qquad \text{(B2)}$$

We note that the V-velocity is related to the U-velocity by the continuity equation (1). Integrating the continuity relation in the normal direction gives

$$V = -\int_0^Y \frac{\partial U}{\partial X}\,dY \qquad \text{(B3)}$$

Then equation (B2) can be written as follows:

$$I_1 = -\int_0^\infty \left(\int_0^Y \frac{\partial U}{\partial X}\,dY\right)\frac{\partial}{\partial Y}\left(\frac{U^{k+1}}{k+1}\right)dY \qquad \text{(B4)}$$

Integrating equation (B4) by parts we obtain

$$I_1 = -\frac{U_\infty^{k+1}}{k+1}\int_0^\infty \frac{\partial U}{\partial X}\,dY + \int_0^\infty \frac{\partial}{\partial X}\left[\frac{U^{k+2}}{(k+1)(k+2)}\right]dY \tag{B5}$$

Next consider the integral

$$I_2 = \int_0^\infty U^k \frac{\partial^2 U}{\partial Y^2}\,dY \tag{B6}$$

For $k = 0$, the integral is evaluated directly and the result is

$$I_2 = \left(\frac{\partial U}{\partial Y}\right)_0^\infty = -\left(\frac{\partial U}{\partial Y}\right)_{Y=0} \qquad k = 0 \tag{B7}$$

For $k \neq 0$, equation (B6) is integrated by parts and we obtain

$$I_2 = -\int_0^\infty kU^{k-1}\left(\frac{\partial U}{\partial Y}\right)^2 dY \qquad k > 0 \tag{B8}$$

Finally, upon substituting the results (B5), (B7), and (B8) into equation (B1), we obtain the following general integral relation:

$$\frac{d}{dX}\int_0^\infty \frac{U}{k+1}\left(U^{k+1} - U_\infty^{k+1}\right)dY$$

$$= \begin{cases} \displaystyle\int_0^\infty U^k \frac{\partial}{\partial t}(U_\infty - U)dY - \nu\left(\frac{\partial U}{\partial Y}\right)_{Y=0} & k = 0 \\ \displaystyle\int_0^\infty U^k \frac{\partial}{\partial t}(U_\infty - U)dY - \nu k\int_0^\infty U^{k-1}\left(\frac{\partial U}{\partial Y}\right)^2 dY & k > 0 \end{cases} \tag{B9}$$

APPENDIX C

DERIVATION OF THE THERMAL INTEGRAL RELATIONS

We multiply the thermal energy equation (4) by a nonnegative power of the dimensionless temperature and integrate the result in the Y-direction from the plate surface to the free stream. The result is

$$\int_0^\infty \theta^k \frac{\partial \theta}{\partial t} dY + \int_0^\infty \theta^k U \frac{\partial \theta}{\partial X} dY + \int_0^\infty \theta^k V \frac{\partial \theta}{\partial Y} dY = \alpha_{th} \int_0^\infty \theta^k \frac{\partial^2 \theta}{\partial Y^2} dY \tag{C1}$$

Consider the following integral:

$$I_3 = \int_0^\infty \theta^k V \frac{\partial \theta}{\partial Y} dY \tag{C2}$$

The transverse velocity V is eliminated by applying the continuity requirement, namely,

$$V = - \int_0^y \frac{\partial U}{\partial X} dY \tag{C3}$$

Then equation (C2) becomes

$$I_3 = - \int_0^\infty \left(\int_0^Y \frac{\partial U}{\partial X} dY \right) \frac{\partial}{\partial Y} \left(\frac{\theta^{k+1}}{k+1} \right) dY \tag{C4}$$

Integration of equation (C4) by parts yields

$$I_3 = \int_0^\infty \frac{1}{k+1} (\theta^{k+1} - 1) \frac{\partial U}{\partial X} dY \tag{C5}$$

Next consider the following:

$$I_4 = \int_0^\infty \theta^k \frac{\partial^2 \theta}{\partial Y^2} dY \tag{C6}$$

For $k = 0$, direct evaluation of the integral gives the result

$$I_4 = -\left(\frac{\partial \theta}{\partial Y}\right)_{Y=0} \qquad k = 0 \tag{C7}$$

For $k \neq 0$, we integrate equation (C6) by parts and the result is as follows:

$$I_4 = -k \int_0^\infty \theta^{k-1} \left(\frac{\partial \theta}{\partial Y}\right)^2 dY \qquad k > 0 \tag{C8}$$

Finally, upon substituting equations (C5), (C7), and (C8) into the integrated energy equation (C1), we obtain the following thermal integral relations:

$$\frac{d}{dX} \int_0^\infty \frac{U}{k+1} (\theta^{k+1} - 1) dY$$

$$= \begin{cases} -\int_0^\infty \frac{\partial \theta}{\partial t} dY - \alpha_{th} \left(\frac{\partial \theta}{\partial Y}\right)_{Y=0} & k = 0 \\ -\int_0^\infty \theta^k \frac{\partial \theta}{\partial t} dY - \alpha_{th} k \int_0^\infty \theta^{k-1} \left(\frac{\partial \theta}{\partial Y}\right)^2 dY & k > 0 \end{cases} \tag{C9}$$

APPENDIX D

METHOD OF SOLUTION FOR SYSTEMS OF NONLINEAR ALGEBRAIC EQUATIONS

The determination of the velocity profile form parameters often requires solving a system of nonlinear algebraic equations of the following form:

$$g_i(A,B,C,\ .\ .\ .) = 0 \tag{D1}$$

In this appendix, the method employed in this work for all such calculations is presented.

First, consider the simple case of one equation of the type (D1); that is,

$$g_1(A) = 0 \tag{D2}$$

In this case, a graph of g_1 against A is constructed and the appropriate root is selected.

Next consider two equations of the following form:

$$g_1(A,B) = 0 \tag{D3}$$

$$g_2(A,B) = 0 \tag{D4}$$

A value of A ($A = A^*$) is picked, and the first equation is evaluated for that A^* for two selected values of B; that is,

$$g_1\left(A^*, B_1\right) = \left(g_1^*\right)_1 \tag{D5}$$

$$g_1\left(A^*, B_2\right) = \left(g_1^*\right)_2 \tag{D6}$$

Referring to figure 33, the value of B for which g_1 is zero (with $A = A^*$) is computed by using the following approximation:

$$B^* = B_1 - \left(g_1^*\right)_1 \frac{B_2 - B_1}{\left(g_1^*\right)_2 - \left(g_1^*\right)_1} \tag{D7}$$

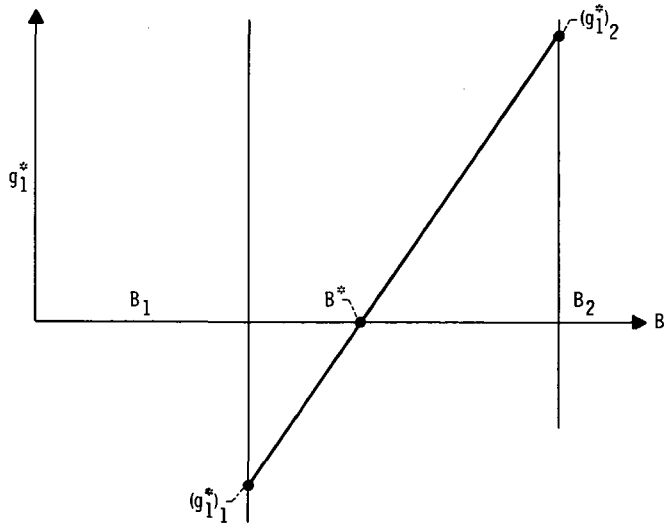

Figure 33. - Linear approximation for a nonlinear function of one variable.

The value of $g_2^*(A^*, B^*)$ is computed and graphed against A^* to determine the solution set (A, B). The process is repeated, with selected values of B chosen closer to the calculated root until the desired accuracy is achieved.

A system of three equations of the type (D1) has the form

$$g_1(A, B, C) = 0 \tag{D8}$$

$$g_2(A, B, C) = 0 \tag{D9}$$

$$g_3(A, B, C) = 0 \tag{D10}$$

A procedure is employed which is an extension of the above procedure for two equations. Assumed values of C are also required, and the linear representations shown in figure 34 are utilized. The resulting equations for B^* and C^* are the following:

$$C^* = C_1 - \left(g_2^*\right)_1 \frac{C_2 - C_1}{\left(g_2^*\right)_2 - \left(g_2^*\right)_1} \tag{D11}$$

$$B^* = B_1^{**} - \left(g_2^*\right)_1 \frac{B_2^{**} - B_1^{**}}{\left(g_2^*\right)_2 - \left(g_2^*\right)_1} \tag{D12}$$

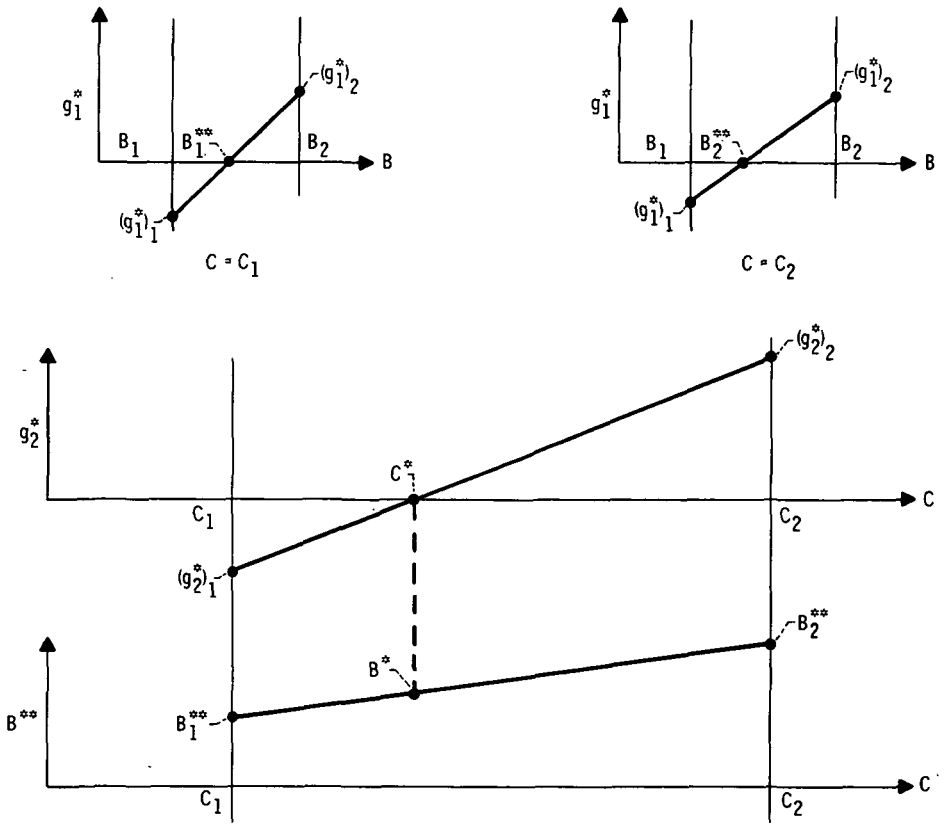

Figure 34. - Linear approximation for a nonlinear function of two variables.

Now, a graph of g_3^* against A^* is constructed to obtain the roots, and the procedure is continued to achieve the desired accuracy.

The procedure is directly extended for larger values of i in equation (D1).

APPENDIX E

DIFFERENTIAL EQUATIONS FOR PROFILE PARAMETERS

In this appendix, we list coefficients of the differential equations of the following form:

$$P_{ij} \frac{d\bar{x}_j}{d\zeta} = R_i \tag{E1}$$

Values corresponding to the first- and second-order flow and temperature approximations are given. All cases utilize the following definitions:

$$\left.\begin{aligned} g_l &= e^{-S_l y} H_{lm} y^{m-1} \\ G(L,M) &= \frac{H_{Ll} H_{Mm} (l + m - 2)!}{(S_L + S_n)^{l+m-1}} \end{aligned}\right\} \text{ sum on } l, m = 1, 2, \ldots, 5 \tag{E2}$$

First-Order Velocity

For the first-order oscillating velocity profiles, the following definitions apply:

$$[g_\ell] = \begin{bmatrix} 1 \\ 1 - u_0 \\ \partial u_0/\partial y \\ 1 - u_1 \\ \partial u_1/\partial_y \\ -\partial u_1/\partial\alpha \\ -\partial u_1/\partial\beta \\ -\partial u_1/\partial\gamma \\ -\partial u_1/\partial\delta \\ -\partial u_0/\partial\zeta \end{bmatrix} \quad [S_\ell] = \begin{bmatrix} 0 \\ A/\zeta \\ A/\zeta \\ \alpha \\ \alpha \\ \alpha \\ \alpha \\ \alpha \\ \alpha \\ A/\zeta \end{bmatrix} \quad [H_{\ell m}] = \begin{bmatrix} 1 & 0 & 0 & 0 & 0 \\ 1 & B/\zeta & C/\zeta^2 & D/\zeta^3 & 0 \\ (A - B)/\zeta & (AB - 2C)/\zeta^2 & (AC - 3D)/\zeta^3 & AD/\zeta^4 & 0 \\ 1 & \beta & \gamma & \delta & 0 \\ \alpha - \beta & \alpha\beta - 2\gamma & \alpha\gamma - 3\delta & \alpha\delta & 0 \\ 0 & -1 & -\beta & -\gamma & -\delta \\ 0 & 1 & 0 & 0 & 0 \\ 0 & 0 & 1 & 0 & 0 \\ 0 & 0 & 0 & 1 & 0 \\ 0 & (A - B)/\zeta^2 & (AB - 2C)/\zeta^3 & (AC - 3D)/\zeta^4 & AD/\zeta^5 \end{bmatrix} \tag{E3}$$

Then, the coefficients of equation (E1) which are utilized in equation (55) are

$$\left.\begin{aligned} P_{1j} &= G(j + 5, 1) - 2G(j + 5, 2) \\ P_{2j} &= 2G(j + 5, 1) - 6G(j + 5, 2) + 3G(j + 5, 2, 2) \\ P_{3j} &= 3G(j + 5, 1) - 12G(j + 5, 2) + 12G(j + 5, 2, 2) - 4G(j + 5, 2, 2, 2) \\ P_{4j} &= 4G(j + 5, 1) - 20G(j + 5, 2) + 30G(j + 5, 2, 2) - 20G(j + 5, 2, 2, 2) \\ &\quad + 5G(j + 5, 2, 2, 2, 2) \end{aligned}\right\} \tag{E4}$$

$$R_1 = 2G(10, 4) - 2\zeta iG(4, 1) + 2\zeta(\alpha - \beta) - F(2, 1) \tag{E5}$$

$$R_2 = 6[G(10, 4) - G(10, 4, 2)] - 4\zeta i[G(4, 1) - G(4, 2)] + 8\zeta^2 G(5, 3) - [4F(2, 1) - 3F(2, 2)] \tag{E6}$$

$$\begin{aligned} R_3 = {} & 12[G(10, 4) - 2G(10, 4, 2) + G(10, 4, 2, 2)] - 6\zeta i[G(4, 1) - 2G(4, 2) + G(4, 2, 2)] \\ & + 12\zeta^2[2G(5, 3) - 2G(5, 3, 2) - G(4, 3, 3)] - [9F(2, 1) \\ & - 12F(2, 2) + 4F(2, 2, 2) - 12\zeta^2 F(3, 3)] \end{aligned} \tag{E7}$$

$$R_4 = 20[G(10,4) - 3G(10,4,2) + 3G(10,4,2,2) - G(10,4,2,2,2)] - 8\zeta i[G(4,1) - 3G(4,2) + 3G(4,2,2) - G(4,2,2,2)] + 48\zeta[G(5,3) - 2G(5,3,2) + G(5,3,2,2) - G(4,3,3) + G(4,3,3,2)] - [16F(2,1) - 30F(2,2) + 20F(2,2,2) - 5F(2,2,2,2) - 48\zeta^2 G(3,3) + 48\zeta^2 G(3,3,2)] \quad \text{(E8)}$$

The F-function definitions corresponding to equation (48) have been retained.

Time-Independent Second-Order Velocity

For the time-independent second-order velocity profile approximations the following arrays are utilized:

$$[g_\ell] = \begin{bmatrix} 1 \\ 1 - u_0 \\ 1 - u_1 \\ 1 - u_1^* \\ \bar{u}_2 \\ \partial u_0/\partial y \\ \partial u_1/\partial y \\ \partial u_1^*/\partial y \\ \partial \bar{u}_2/\partial y \\ \partial u_0/\partial \zeta \\ \partial u_1/\partial \zeta \\ \partial u_1^*/\partial \zeta \\ \partial \bar{u}_2/\partial \varphi \\ \partial \bar{u}_2/\partial \psi \\ \partial \bar{u}_2/\partial \mu \\ \partial \bar{u}_2/\partial \lambda \end{bmatrix} \quad [S_\ell] = \begin{bmatrix} 0 \\ A/\zeta \\ \alpha \\ \alpha^* \\ \varphi \\ A/\zeta \\ \alpha \\ \alpha^* \\ \varphi \\ A/\zeta \\ \alpha \\ \alpha^* \\ \varphi \\ \varphi \\ \varphi \\ \varphi \end{bmatrix}$$

$$[H_{\ell m}] = \begin{bmatrix} 1 & 0 & 0 & 0 & 0 \\ 1 & B/\zeta & C/\zeta^2 & D/\zeta^3 & 0 \\ 1 & \beta & \gamma & \delta & 0 \\ 1 & \beta^* & \gamma^* & \delta^* & 0 \\ 0 & \psi & \mu & \lambda & 0 \\ (A-B)/\zeta & (AB-2C)/\zeta^2 & (AC-3D)/\zeta^3 & AD/\zeta^4 & 0 \\ \alpha - \beta & \alpha\beta - 2\gamma & \alpha\gamma - 3\delta & \alpha\delta & 0 \\ \alpha^* - \beta^* & \alpha^*\beta^* - 2\gamma^* & \alpha^*\gamma^* - 3\delta^* & \alpha^*\delta^* & 0 \\ \psi & 2\mu - \varphi\psi & 3\lambda - \varphi\mu & -\varphi\lambda & 0 \\ 0 & (B-A)/\zeta^2 & (2C-AB)/\zeta^3 & (3D-AC)/\zeta^4 & -AD/\zeta^5 \\ 0 & (\alpha' - \beta') & (\alpha'\beta - \gamma') & (\alpha'\gamma - \delta') & (\alpha'\delta) \\ 0 & (\alpha' - \beta')^* & (\alpha'\beta - \gamma')^* & (\alpha'\gamma - \delta')^* & (\alpha'\delta)^* \\ 0 & 0 & -\psi & -\mu & -\lambda \\ 0 & 1 & 0 & 0 & 0 \\ 0 & 0 & 1 & 0 & 0 \\ 0 & 0 & 0 & 1 & 0 \end{bmatrix} \quad \text{(E9)}$$

Then, the coefficients of equation (73) have the values

$$\left.\begin{aligned} P_{1j} &= [G(j+12,1) - 2G(j+12,2)] \\ P_{2j} &= \frac{1}{2}[2G(j+12,1) - 6G(j+12,2) + 3G(j+12,2,2)] \\ P_{3j} &= \frac{1}{3}[3G(j+12,1) - 12G(j+12,2) + 12G(j+12,2,2) - 4G(j+12,2,2,2)] \\ P_{4j} &= \frac{1}{4}[4G(j+12,1) - 20G(j+12,2) + 30G(j+12,2,2) \\ &\qquad - 20G(j+12,2,2,2) + 5G(j+12,2,2,2,2)] \end{aligned}\right\} \quad \text{(E10)}$$

$$R_1 = -2\xi\psi - 2G(10,5) + \frac{1}{2}\,Re\,\{G(11,4) - G(12,1) + G(12,3)\} \quad \text{(E11)}$$

$$\begin{aligned} R_2 = -3[G(10,5) - G(10,5,2)] - \xi\,\mathcal{I}\{G(3,1)\} - 4\xi G(9,6) - \xi\,Re\,\{G(8,7)\} - \frac{1}{4}\,Re\,\{2G(11,1) \\ + 2G(10,1) + 3[G(12,1) - G(12,3) - G(12,2) + G(12,3,2) - G(11,4) \\ - G(11,2) + G(11,4,2) - G(10,4) - G(10,3) + G(10,4,3)]\} \end{aligned} \quad \text{(E12)}$$

$$\begin{aligned} R_3 = -4[G(10,5) - 2G(10,5,2) + G(10,5,2,2)] - 2\xi\,\mathcal{I}\{G(3,1) - G(3,2)\} - 8\xi[G(9,6) \\ - G(9,6,2)] - 2\xi\,Re\,\{G(8,7) - G(8,7,2) + G(8,6) - G(8,6,3) + G(7,6) - G(7,6,4) \\ + 2G(6,6,5)\} - Re\left\{\frac{3}{2}G(10,1) - 2G(10,2) - 2G(10,3) - 2G(10,4) + 2G(10,4,3)\right. \\ + 2G(10,4,2) + 2G(10,3,2) - 2G(10,4,3,2) + G(12,1) - G(12,3) - 2G(12,2) \\ + 2G(12,3,2) + G(12,2,2) - G(12,3,2,2) + \frac{1}{2}G(11,1) - G(11,4) - 2G(11,2) \\ \left. + 2G(11,4,2) + G(11,2,2) - G(11,4,2,2)\right\} \end{aligned} \quad \text{(E13)}$$

$$R_4 = -5[G(10,5) - 3G(10,5,2) + 3G(10,5,2,2) - G(10,5,2,2,2)] - 3\xi\mathcal{I}\{G(3,1) - 2G(3,2)$$

$$+ G(3,2,2)\} - 12\xi[G(9,6) - 2G(9,6,2) + G(9,6,2,2) + G(6,6,5) - G(6,6,5,2)]$$

$$- 3\xi\,\mathcal{R}e\,\{[G(8,7) - 2G(8,7,2) + G(8,7,2,2)] + 2[G(8,6) - G(8,6,2)$$

$$- G(8,6,3) + G(8,6,3,2)] + 2[G(7,6) - G(7,6,2) - G(7,6,4) + G(7,6,4,2)]$$

$$+ [G(6,6) - G(6,6,4) - G(6,6,3) + G(6,6,4,3)]\} - \frac{5}{4}\,\mathcal{R}e\Big\{3[G(10,1)$$

$$- 2G(10,2) + G(10,2,2) - G(10,3) + 2G(10,3,2) - G(10,3,2,2) - G(10,4)$$

$$+ 2G(10,4,2) - G(10,4,2,2) + G(10,4,3) - G(10,4,3,2) + G(10,4,3,2,2)]$$

$$+ G(12,1) - 3G(12,2) + 3G(12,2,2) - G(12,2,2,2) - G(12,3) + 3G(12,3,2)$$

$$- 3G(12,3,2,2) + G(12,3,2,2,2) - \frac{3}{5}G(11,1) - 3G(11,2) + 3G(11,2,2)$$

$$- G(11,2,2,2) - G(11,3) + 3G(11,3,2) - 3G(11,3,2,2) + G(11,3,2,2,2)\Big\} \tag{E14}$$

First-Order Temperature

The first-order temperature profile form factor calculation is based on the following definitions:

$$[G_\ell] = \begin{bmatrix} 1 \\ 1 - u_0 \\ \partial u_0/\partial y \\ \partial u_0/\partial \zeta \\ 1 - u_1 \\ \partial u_1/\partial y \\ \partial u_1/\partial \zeta \\ 1 - \theta_0 \\ \partial \theta_0/\partial y \\ \partial \theta_0/\partial \zeta \\ \theta_1 \\ \partial \theta_1/\partial y \\ \partial \theta_1/\partial \bar{\alpha} \\ \partial \theta_1/\partial \bar{\beta} \\ \partial \theta_1/\partial \bar{\gamma} \\ \partial \theta_1/\partial \bar{\delta} \end{bmatrix} \quad [S_\ell] = \begin{bmatrix} 0 \\ A/\zeta \\ A/\zeta \\ A/\zeta \\ \alpha \\ \alpha \\ \alpha \\ \bar{A}/\zeta \\ \bar{A}/\zeta \\ \bar{A}/\zeta \\ \bar{\alpha} \\ \bar{\alpha} \\ \bar{\alpha} \\ \bar{\alpha} \\ \bar{\alpha} \\ \bar{\alpha} \end{bmatrix} \quad [H_{ij}] = \begin{bmatrix} 1 & 0 & 0 & 0 & 0 \\ 1 & B/\zeta & C/\zeta^2 & D/\zeta^3 & 0 \\ (A - B)/\zeta & (AB - 2C)/\zeta^2 & (AC - 3D)/\zeta^3 & AD/\zeta^4 & 0 \\ 0 & -(A - B)/\zeta^2 & -(AB - 2C)/\zeta^3 & -(AC - 3D)/\zeta^4 & -AD/\zeta^5 \\ 1 & \beta & \gamma & \delta & 0 \\ (\alpha - \beta) & (\alpha\beta - 2\gamma) & (\alpha\gamma - 3\delta) & \alpha\delta & 0 \\ 0 & (\alpha' - \beta') & (\alpha'\beta - \gamma') & (\alpha'\gamma - \delta') & \alpha'\delta \\ 1 & \bar{B}/\zeta & \bar{C}/\zeta^3 & \bar{D}/\zeta^3 & 0 \\ (\bar{A} - \bar{B})/\zeta & (\overline{AB} - 2\bar{C})/\zeta^2 & (\overline{AC} - 3\bar{D})/\zeta^3 & \overline{AD}/\zeta^4 & 0 \\ 0 & -(\bar{A} - \bar{B})/\zeta^2 & -(\overline{AB} - 2\bar{C})/\zeta^3 & -(\overline{AC} - 3\bar{D})/\zeta^4 & -\overline{AD}/\zeta^5 \\ 0 & \bar{\beta} & \bar{\gamma} & \bar{\delta} & 0 \\ \bar{\beta} & 2\bar{\gamma} - \overline{\alpha\beta} & 2\bar{\delta} - \overline{\alpha\gamma} & -\overline{\alpha\delta} & 0 \\ 0 & 0 & -\bar{\beta} & -\bar{\gamma} & -\bar{\delta} \\ 0 & 1 & 0 & 0 & 0 \\ 0 & 0 & 1 & 0 & 0 \\ 0 & 0 & 0 & 1 & 0 \end{bmatrix} \tag{E15}$$

With these definitions, the terms in equation (100) are

$$\left.\begin{aligned} P_{1j} &= [G(j + 12, 1) - G(j + 12, 2)] \\ P_{2j} &= 2[G(j + 12, 1) - G(j + 12, 2) - G(j + 12, 8) + G(j + 12, 8, 2)] \\ P_{3j} &= 3[G(j + 12, 1) - G(j + 12, 2) - 2G(j + 12, 8) + 2G(j + 12, 8, 2) \\ &\quad + G(j + 12, 8, 8) - G(j + 12, 8, 8, 2)] \\ P_{4j} &= 4[G(j + 12, 1) - G(j + 12, 2) - 3G(j + 12, 8) + 3G(j + 12, 8, 2) \\ &\quad + 3G(j + 12, 8, 8) - 3G(j + 12, 8, 8, 2) - G(j + 12, 8, 8, 8) \\ &\quad + G(j + 12, 8, 8, 8, 2)] \end{aligned}\right\} \tag{E16}$$

$$R_1 = -\left(\frac{2\zeta\bar{\beta}}{Pr}\right) - 2\zeta i[G(11,1)] - [G(11,4) + G(10,1) - G(10,5) - G(8,7)] \tag{E17}$$

$$R_2 = -\left(\frac{8\zeta}{Pr}\right)[G(12,9)] - 4\zeta i[G(11,1) - G(11,8)] - 2[G(11,10) - G(11,10,2) + G(11,4)$$

$$- G(11,8,4) + G(10,1) - G(10,8) - G(10,5)$$

$$+ G(10,8,5)] + [G(8,8,7) - 2G(8,7)] \tag{E18}$$

$$R_3 = -\left(\frac{12\zeta}{Pr}\right)[2G(12,9) - 2G(12,9,8) + G(11,9,9)] - 6\zeta i[G(11,1) - 2G(11,8) + G(11,8,8)]$$

$$- 6[G(11,10) - G(11,10,2) - G(11,10,8) + G(11,10,8,2)] - 3[G(11,4) + G(10,1)$$

$$- G(10,5) - 2G(11,8,4) - 2G(10,8) + 2G(10,8,5) + G(11,8,8,4) + G(10,8,8)$$

$$- G(10,8,8,5)] - [G(8,8,8,7) - 3G(8,8,7) + 3G(8,7)] \tag{E19}$$

$$R_4 = -\left(\frac{48\zeta}{Pr}\right)[G(12,9) - 2G(12,9,8) + G(12,9,8,8) + G(11,9,9) - G(11,9,9,8)]$$

$$- 8\zeta i[G(11,1) - 3G(11,8) + 3G(11,8,8) - G(11,8,8,8)] - 12[G(11,10) - 2G(11,10,8)$$

$$+ G(11,10,8,8) - G(11,10,2) + 2G(11,10,8,2) - G(11,10,8,8,2)] - 4[G(10,1)$$

$$- 3G(10,8) + 3G(10,8,8) - G(10,8,8,8) - G(10,5) + 3G(10,8,5) - 3G(10,8,8,5)$$

$$+ G(10,8,8,8,5) - G(11,4) - 3G(11,8,4) + 3G(11,8,8,4) - G(11,8,8,8,4)]$$

$$- [G(8,8,8,8,7) - 4G(8,8,8,7) + 6G(8,8,7) - 4G(8,7)] \tag{E20}$$

Time-Independent Second-Order Temperature

The required notation for the second-order temperature equation is

$$
[g_\ell] = \begin{bmatrix}
1 \\
1 - u_0 \\
1 - u_1 \\
\bar{u}_2 \\
1 - \theta_0 \\
\theta_1 \\
\theta_1^* \\
\bar{\theta}_2 \\
\partial\theta_0/\partial y \\
\partial\theta_1/\partial y \\
\partial\theta_1^*/\partial y \\
\partial\bar{\theta}_2/\partial y \\
\partial u_0/\partial\zeta \\
\partial u_1/\partial\zeta \\
\partial\bar{u}_2/\partial\zeta \\
\partial\theta_0/\partial\zeta \\
\partial\theta_1/\partial\zeta \\
\partial\theta_1^*/\partial\zeta \\
\partial\bar{\theta}_2/\partial\bar{\varphi} \\
\partial\bar{\theta}_2/\partial\bar{\psi} \\
\partial\bar{\theta}_2/\partial\bar{\mu} \\
\partial\bar{\theta}_2/\partial\bar{\lambda}
\end{bmatrix}
\quad
[S_\ell] = \begin{bmatrix}
0 \\
A/\zeta \\
\alpha \\
\varphi \\
\bar{A}/\zeta \\
\bar{\alpha} \\
\bar{\alpha}^* \\
\bar{\varphi} \\
\bar{A}/\zeta \\
\bar{\alpha} \\
\bar{\alpha}^* \\
\bar{\varphi} \\
A/\zeta \\
\alpha \\
\varphi \\
\bar{A}/\zeta \\
\bar{\alpha} \\
\bar{\alpha}^* \\
\bar{\varphi} \\
\bar{\varphi} \\
\bar{\varphi} \\
\bar{\varphi}
\end{bmatrix}
$$

$$
[H_{\ell m}] = \begin{bmatrix}
1 & 0 & 0 & 0 & 0 \\
1 & B/\zeta & C/\zeta^2 & D/\zeta^3 & 0 \\
1 & \beta & \gamma & \delta & 0 \\
0 & \psi & \mu & \lambda & 0 \\
1 & \bar{B}/\zeta & \bar{C}/\zeta^2 & \bar{D}/\zeta^3 & 0 \\
0 & \bar{\beta} & \bar{\gamma} & \bar{\delta} & 0 \\
0 & \bar{\beta}^* & \bar{\gamma}^* & \bar{\delta}^* & 0 \\
0 & \bar{\psi} & \bar{\mu} & \bar{\lambda} & 0 \\
(\bar{A} - \bar{B})/\zeta & (\overline{AB} - 2\bar{C})/\zeta^2 & (\overline{AC} - 3\bar{D})/\zeta^3 & \overline{AD}/\zeta^4 & 0 \\
\bar{\beta} & 2\bar{\gamma} - \overline{\alpha\beta} & 3\bar{\delta} - \overline{\alpha\gamma} & -\overline{\alpha\delta} & 0 \\
\bar{\beta}^* & 2\bar{\gamma}^* - \bar{\alpha}^*\bar{\beta}^* & 3\bar{\delta}^* - \bar{\alpha}^*\bar{\gamma}^* & -\bar{\alpha}^*\bar{\delta}^* & 0 \\
\bar{\psi} & 2\bar{\mu} - \overline{\varphi\psi} & 3\bar{\lambda} - \overline{\varphi\mu} & -\overline{\varphi\lambda} & 0 \\
0 & (B - A)/\zeta^2 & (2C - AB)/\zeta^3 & (3D - AC)/\zeta^4 & -AD/\zeta^5 \\
0 & \alpha' - \beta' & \alpha'\beta - \gamma' & \alpha'\gamma - \delta' & \alpha'\delta \\
0 & \psi' & \mu' - \varphi'\psi & \lambda' - \varphi'\mu & -\varphi'\lambda \\
0 & (\bar{B} - \bar{A})/\zeta^2 & (2\bar{C} - \overline{AB})/\zeta^3 & (3\bar{D} - \overline{AC})/\zeta^4 & -\overline{AD}/\zeta^5 \\
0 & \bar{\beta}' & \bar{\gamma}' - \bar{\alpha}'\bar{\beta} & \bar{\delta}' - \bar{\alpha}'\bar{\gamma} & -\bar{\alpha}'\bar{\delta} \\
0 & (\bar{\beta}')^* & (\bar{\gamma}' - \bar{\alpha}'\bar{\beta})^* & (\delta' - \alpha'\gamma)^* & (-\alpha'\delta)^* \\
0 & 0 & -\bar{\psi} & -\bar{\mu} & -\bar{\lambda} \\
0 & 1 & 0 & 0 & 0 \\
0 & 0 & 1 & 0 & 0 \\
0 & 0 & 0 & 1 & 0
\end{bmatrix}
\qquad \text{(E21)}
$$

Then, the coefficients required for equation (117) are

$$\left.\begin{aligned}
P_{1j} &= G(j+18,1) - G(j+18,2) \\
P_{2j} &= P_{1j} - G(j+18,5) + G(j+18,5,2) \\
P_{3j} &= P_{1j} - 2G(j+18,5) + 2G(j+18,5,2) - G(j+18,5,5) \\
&\quad - G(j+18,5,5,2) \\
P_{4j} &= P_{1j} - 3G(j+18,5) + 3G(j+18,5,2) + 3G(j+18,5,5) \\
&\quad - 3G(j+18,5,5,2) - G(j+18,5,5,5) \\
&\quad + G(j+18,5,5,5,2)
\end{aligned}\right\} \qquad \text{(E22)}$$

$$R_1 = \left(\frac{-2\zeta\bar{\psi}}{Pr}\right) - [G(13,8)] - [G(16,4) - G(15,5) + 0.5\,G(14,7) + 0.5\,G(18,1) - 0.5\,G(18,3)] \qquad \text{(E23)}$$

$$\begin{aligned}
R_2 = \left(\frac{-4\zeta}{Pr}\right)&[G(12,9) + 0.25\,G(11,10)] - [G(13,8) - G(13,8,5) + G(16,8) - G(16,8,2)] \\
&- [0.5\,G(15,5,5) - G(15,5) + G(16,4) - G(16,5,4)] - 0.5[G(14,7) - G(14,7,5) \\
&+ G(18,1) - G(18,3) - G(18,5) + G(18,5,3) + G(16,7) - G(16,7,3)] \\
&- 0.25[G(13,7,6) + G(17,7) - G(17,7,2) + G(18,6) - G(18,6,2)]
\end{aligned} \qquad \text{(E24)}$$

$$R_3 = \left(\frac{-2\zeta}{Pr}\right)[4G(12,9) - 4G(12,9,5) + G(11,9,6) + G(10,9,7) + 2G(9,9,8) + G(11,10)$$

$$- G(11,10,5)] - [G(13,8) - 2G(13,8,5) + G(13,8,5,5) + 2G(16,8) - 2G(16,8,5)$$

$$- 2G(16,8,2) + G(16,8,5,2)] + \frac{1}{3}[G(15,5,5,5) - 3G(15,5,5) + 3G(15,5)]$$

$$- [G(16,4) - 2G(16,5,4) + G(16,5,5,4) + G(16,7) - G(16,7,5) - G(16,7,3)$$

$$+ G(16,7,5,3)] - 0.5[G(14,7) - 2G(14,7,5) + G(14,7,5,5) + G(18,1)$$

$$- 2G(18,5) + G(18,5,5) - G(18,3) + 2G(18,5,3) - G(18,5,5,3) + G(13,7,6)$$

$$- G(13,7,6,5) + G(17,7) - G(17,7,5) - G(17,7,2) + G(17,7,5,2) + G(18,6)$$

$$- G(18,6,5) - G(18,6,2) + G(18,6,5,2) + G(16,7,6) - G(16,7,6,2)] \qquad (E25)$$

$$R_4 = \left(\frac{-3\zeta}{Pr}\right)[4G(12,9) - 8G(12,9,5) + 4G(12,9,5,5) + 2G(11,9,6) - 2G(11,9,6,5)$$

$$+ 2G(10,9,7) - 2G(10,9,7,5) + 4G(9,9,8) - 4G(9,9,8,5) + G(11,10) - 2G(11,10,5)$$

$$+ G(11,10,5,5) + G(9,9,7,6)] - [G(13,8) - 3G(13,8,5) + 3G(13,8,5,5)$$

$$- G(13,8,5,5,5)] - 3[G(16,8) - 2G(16,8,5) + G(16,8,5,5) - G(16,8,2)$$

$$+ 2G(16,8,5,2) - G(10,8,5,5,2)] - \frac{1}{4}\Big\{[F(15,5,5,5,5) - 4F(15,5,5,5) + 6F(15,5,5)$$

$$- 4F(15,5)] + 4[G(16,4) - 3G(16,5,4) + 3G(16,5,5,4) - G(16,5,5,5,4)] + 2[G(14,7)$$

$$- 3G(14,7,5) + 3G(14,7,5,5) - G(14,7,5,5,5) + G(18,1) - 3G(18,5) + 3G(18,5,5)$$

$$- G(18,5,5,5) - G(18,3) + 3G(18,5,3) + 3G(18,5,5,3) + G(18,5,5,5,3)]$$

$$+ 6[G(16,7) - 2G(16,7,5) + G(16,7,5,5) - G(16,7,3) + 2G(16,7,5,3)$$

$$- G(16,7,5,5,3) + G(16,7,6) - G(16,7,6,5) - G(16,7,6,2) + G(17,7,6,5,2)]$$

$$+ 3[G(13,7,6) - 2G(13,7,6,5) + G(13,7,6,5,5) + G(17,7) - 2G(17,7,5)$$

$$+ G(17,7,5,5) - G(17,7,2) + 2G(17,7,5,2) - G(17,7,5,5,2) + G(18,6)$$

$$- 2G(18,6,5) + G(18,6,5,5) - G(18,6,2) + G(18,6,5,2) - G(18,6,5,5,2)]\Big\}$$

(E26)

APPENDIX F

FOURTH-ORDER RUNGE-KUTTA INTEGRATION FORMULAS

In this appendix we list the Runge-Kutta formulas which were used to solve the systems of coupled first-order ordinary differential equations of the form

$$\frac{d\alpha}{d\zeta} = \pi_1(\alpha, \beta, \gamma, \delta, \zeta) \tag{F1}$$

$$\frac{d\beta}{d\zeta} = \pi_2(\alpha, \beta, \gamma, \delta, \zeta) \tag{F2}$$

$$\frac{d\gamma}{d\zeta} = \pi_3(\alpha, \beta, \gamma, \delta, \zeta) \tag{F3}$$

$$\frac{d\delta}{d\zeta} = \pi_4(\alpha, \beta, \gamma, \delta, \zeta) \tag{F4}$$

The initial conditions are as follows:

$$\alpha(\zeta_0) = \alpha_0 \tag{F5}$$

$$\beta(\zeta_0) = \beta_0 \tag{F6}$$

$$\gamma(\zeta_0) = \gamma_0 \tag{F7}$$

$$\delta(\zeta_0) = \delta_0 \tag{F8}$$

We apply a step-by-step procedure starting at ζ_0 and apply the following formulas (cf. Levy and Baggott (ref. 15)):

$$\alpha_{n+1} = \alpha_n + \frac{1}{6}(k_0 + 2k_1 + 2k_2 + k_3) \tag{F9}$$

$$\beta_{n+1} = \beta_n + \frac{1}{6}(l_0 + 2l_1 + 2l_2 + l_3) \tag{F10}$$

$$\gamma_{n+1} = \gamma_n + \frac{1}{6}(m_0 + 2m_1 + 2m_2 + m_3) \tag{F11}$$

$$\delta_{n+1} = \delta_n + \frac{1}{6}(n_0 + 2n_1 + 2n_2 + n_3) \tag{F12}$$

where

$$k_0 = \Delta\, \pi_1(\alpha_n, \beta_n, \gamma_n, \delta_n, \zeta_n) \tag{F13}$$

$$k_1 = \Delta\, \pi_1\left(\alpha_n + \frac{1}{2}k_0,\ \beta_n + \frac{1}{2}l_0,\ \gamma_n + \frac{1}{2}m_0,\ \delta_n + \frac{1}{2}n_0,\ \zeta_n + \frac{1}{2}\Delta\right) \tag{F14}$$

$$k_2 = \Delta\, \pi_1\left(\alpha_n + \frac{1}{2}k_1,\ \beta_n + \frac{1}{2}l_1,\ \gamma_n + \frac{1}{2}m_1,\ \delta_n + \frac{1}{2}n_1,\ \zeta_n + \frac{1}{2}\Delta\right) \tag{F15}$$

$$k_3 = \Delta\, \pi_1(\alpha_n + k_2,\ \beta_n + l_2,\ \gamma_n + m_2,\ \delta_n + n_2,\ \zeta_n + \Delta) \tag{F16}$$

$$l_0 = \Delta\, \pi_2(\alpha_n, \beta_n, \gamma_n, \delta_n, \zeta_n) \tag{F17}$$

$$l_1 = \Delta\, \pi_2\left(\alpha_n + \frac{1}{2}k_0,\ \beta_n + \frac{1}{2}l_0,\ \gamma_n + \frac{1}{2}m_0,\ \delta_n + \frac{1}{2}n_0,\ \zeta_n + \frac{1}{2}\Delta\right) \tag{F18}$$

$$l_2 = \Delta\, \pi_2\left(\alpha_n + \frac{1}{2}k_1,\ \beta_n + \frac{1}{2}l_1,\ \gamma_n + \frac{1}{2}m_1,\ \delta_n + \frac{1}{2}n_1,\ \zeta_n + \frac{1}{2}\Delta\right) \tag{F19}$$

$$l_3 = \Delta\, \pi_2(\alpha_n + k_2,\ \beta_n + l_2,\ \gamma_n + m_2,\ \delta_n + n_2,\ \zeta_n + \Delta) \tag{F20}$$

$$m_0 = \Delta\, \pi_3(\alpha_n, \beta_n, \gamma_n, \delta_n, \zeta_n) \tag{F21}$$

$$m_1 = \Delta\, \pi_3\left(\alpha_n + \frac{1}{2}k_0,\ \beta_n + \frac{1}{2}l_0,\ \gamma_n + \frac{1}{2}m_0,\ \delta_n + \frac{1}{2}n_0,\ \zeta_n + \frac{1}{2}\Delta\right) \tag{F22}$$

$$m_2 = \Delta\, \pi_3\left(\alpha_n + \frac{1}{2}k_1,\ \beta_n + \frac{1}{2}l_1,\ \gamma_n + \frac{1}{2}m_1,\ \delta_n + \frac{1}{2}n_1,\ \zeta_n + \frac{1}{2}\Delta\right) \tag{F23}$$

$$m_3 = \Delta\, \pi_3(\alpha_n + k_2,\ \beta_n + l_2,\ \gamma_n + m_2,\ \delta_n + n_2,\ \zeta_n + \Delta) \tag{F24}$$

$$n_0 = \Delta\, \pi_4(\alpha_n, \beta_n, \gamma_n, \delta_n, \zeta_n) \tag{F25}$$

$$n_1 = \Delta\, \pi_4\left(\alpha_n + \frac{1}{2}k_0,\ \beta_n + \frac{1}{2}l_0,\ \gamma_n + \frac{1}{2}m_0,\ \delta_n + \frac{1}{2}n_0,\ \zeta_n + \frac{1}{2}\Delta\right) \tag{F26}$$

$$n_2 = \Delta\, \pi_4\left(\alpha_n + \frac{1}{2}k_1,\ \beta_n + \frac{1}{2}l_1,\ \gamma_n + \frac{1}{2}m_1,\ \delta_n + \frac{1}{2}n_1,\ \zeta_n + \frac{1}{2}\Delta\right) \tag{F27}$$

$$n_3 = \Delta\, \pi_4(\alpha_n + k_2,\ \beta_n + l_2,\ \gamma_n + m_2,\ \delta_n + n_2,\ \zeta_n + \Delta) \tag{F28}$$

In the preceding fourth-order formulas given we have defined

$$\Delta = \zeta_{n+1} - \zeta_n \tag{F29}$$

REFERENCES

1. Lighthill, M. J : The Response of Laminar Skin Friction and Heat Transfer to Fluctuations in the Stream Velocity. Proc. Roy. Soc. (London), Ser. A, vol. 224, no. 1156, June 9, 1954, pp. 1-23.

2. Illingworth, C. R.: The Effects of a Sound Wave on the Compressible Boundary Layer on a Flat Plate. J. Fluid Mech., vol. 3, pt. 5, Feb. 1958, pp. 471-493.

3. Moore, Franklin K.: Unsteady Laminar Boundary-Layer Flow. NACA TN 2471, 1951.

4. Ostrach, Simon: Compressible Laminar Boundary Layer and Heat Transfer for Unsteady Motions of a Flat Plate. NACA TN 3569, 1955.

5. Moore, Franklin K.; and Ostrach, Simon: Average Properties of Compressible Laminar Boundary Layer on Flat Plate with Unsteady Flight Velocity. NACA TN 3886, 1956.

6. Stuart, J. T.: A Solution of the Navier-Stokes and Energy Equations Illustrating the Response of Skin Friction and Temperature of an Infinite Plate Thermometer to Fluctuations in the Stream Velocity. Proc. Roy. Soc. (London), Ser. A, vol. 231, no. 1184, July 19, 1955, pp. 116-130.

7. Gersten, K.: Heat Transfer in Laminar Boundary Layers with Oscillating Outer Flow. Recent Developments in Boundary Layer Research. Part 1. AGARDograph 97, Pt. 1, 1965, pp. 423-475.

8. Nickerson, Richard J.: The Effect of Free-Stream Oscillations on the Laminar Boundary Layers on a Flat Plate. Heat Transfer Lab., Massachusetts Inst. Tech. (WADC-TR-57-481), Dec. 1958.

9. Miller, Roy W.: Analysis of Unsteady Laminar Boundary Layer Flow by an Integral Method. NASA TM X-67852, 1971.

10. Miller, R. W.; and Han, L. S.: Analysis of Unsteady Laminar Boundary Layer Flow by an Integral Method. J. Basic Eng., Jan. 1973, pp. 1-11.

11. Walz, Alfred: Boundary Layers of Flow and Temperature. MIT Press, 1969.

12. Schlichting, Hermann (J. Kestin, trans.): Boundary Layer Theory. Fourth ed., McGraw-Hill Book Co., Inc., 1960.

13. Hill, P. G.; and Stenning, A. H.: Laminar Boundary Layers on Oscillatory Flow. J. Basic Eng., vol. 82, no. 3, Sept. 1960, pp. 593-608.

14. Rott, Nicholas: Theory of Time-Dependent Laminar Flows. Theory of Laminar Flows. F. K. Moore, ed., Princeton Univ. Press, 1964, pp. 395-438.

15. Levy, Hyman; and Baggott, E. A.: Numerical Solutions of Differential Equations. Dover Publications, 1950.

NASA-Langley, 1972 —— 33 E-6876

NATIONAL AERONAUTICS AND SPACE ADMINISTRATION
WASHINGTON, D.C. 20546

OFFICIAL BUSINESS
PENALTY FOR PRIVATE USE $300

SPECIAL FOURTH-CLASS RATE BOOK

POSTAGE AND FEES PAID
NATIONAL AERONAUTICS AND SPACE ADMINISTRATION
451

U.S.MAIL

POSTMASTER : If Undeliverable (Section 158 Postal Manual) Do Not Return

"The aeronautical and space activities of the United States shall be conducted so as to contribute . . . to the expansion of human knowledge of phenomena in the atmosphere and space. The Administration shall provide for the widest practicable and appropriate dissemination of information concerning its activities and the results thereof."

—NATIONAL AERONAUTICS AND SPACE ACT OF 1958

NASA SCIENTIFIC AND TECHNICAL PUBLICATIONS

TECHNICAL REPORTS: Scientific and technical information considered important, complete, and a lasting contribution to existing knowledge.

TECHNICAL NOTES: Information less broad in scope but nevertheless of importance as a contribution to existing knowledge.

TECHNICAL MEMORANDUMS: Information receiving limited distribution because of preliminary data, security classification, or other reasons. Also includes conference proceedings with either limited or unlimited distribution.

CONTRACTOR REPORTS: Scientific and technical information generated under a NASA contract or grant and considered an important contribution to existing knowledge.

TECHNICAL TRANSLATIONS: Information published in a foreign language considered to merit NASA distribution in English.

SPECIAL PUBLICATIONS: Information derived from or of value to NASA activities. Publications include final reports of major projects, monographs, data compilations, handbooks, sourcebooks, and special bibliographies.

TECHNOLOGY UTILIZATION PUBLICATIONS: Information on technology used by NASA that may be of particular interest in commercial and other non-aerospace applications. Publications include Tech Briefs, Technology Utilization Reports and Technology Surveys.

Details on the availability of these publications may be obtained from:

SCIENTIFIC AND TECHNICAL INFORMATION OFFICE

NATIONAL AERONAUTICS AND SPACE ADMINISTRATION

Washington, D.C. 20546